# RHEOLOGICAL AND ABRASION RESISTANT PROPERTIES OF TRANSPARENT POLYMER/SILICATE NANOCOMPOSITE COATINGS

By

JENNIFER MARIE BRANDT

A THESIS PRESENTED TO THE GRADUATE SCHOOL
OF THE UNIVERSITY OF FLORIDA IN PARTIAL FULFILLMENT
OF THE REQUIREMENTS FOR THE DEGREE OF
MASTER OF SCIENCE

UNIVERSITY OF FLORIDA

2005

This document is dedicated to Michael Sachs, Kristin Brandt, and my parents, David and Marie Brandt.

ACKNOWLEDGMENTS

I would like to express my appreciation to my committee chair and advisor, Dr. Abbas Zaman. I would also like to thank Dr. Zaman's graduate student, Heather Trotter, and his group of undergraduate students. Special thanks go to Betty Arias for her hard work on may aspects of this work.

I would like to thank my committee members Dr. Charles Beatty and Dr. Susan Sinnott for their advice and support.

I would also like to thank the students and staff of the Particle Engineering Research Center at the University of Florida.

I would like to thank the Air Force for their financial support.

TABLE OF CONTENTS

page

LIST OF TABLES

Table page

LIST OF FIGURES

Abstract of Thesis Presented to the Graduate School
of the University of Florida in Partial Fulfillment of the
Requirements for the Degree of Master of Science

RHEOLOGICAL AND ABRASION RESISTANT PROPERTIES OF TRANSPARENT POLYMER/SILICATE NANOCOMPOSITE COATINGS

By

Jennifer Marie Brandt

May 2005

Chair: Abbas A. Zaman
Major Department: Materials Science and Engineering

Polymer nanocomposite thin films were cast from colloidal dispersions of polyvinyl alcohol and Laponite JS. Rheological studies were performed to determine the effect of shear rate and small amplitude oscillatory shear on the colloidal dispersions. Structural development of the dispersions was determined as a function of polymer concentration and Laponite solids loading. Solution casting of the dispersions resulted in transparent coatings with strong adhesion to a glass substrate. Scanning electron microscopy revealed the presence of flocculated particle clusters in the films.

Adhesion of the films to a hydrophobic polymer interlayer was achieved by activating the surface of the polymer using wet-chemical treatments. The treatments included mixtures of sulfuric and nitric acid and several silane coupling agents. The success of the treatments was determined using FTIR-ATR surface analysis. Highly concentrated acid treatments and several coupling agents were determined to be successful in surface modification of the polymer.

To determine the abrasion resistance of the nanocomposite films, a Taber linear abrader was used to abrade the samples and weight loss was observed. Samples with single, double, and triple coatings of film with solids loadings of 40, 50, and 60 wt% were cast onto glass slides and abraded by the instrument. Of these samples, the double-coated films lost the least weight when compared to the glass slide. The films containing high solids loadings had the best performance and the most reproducibility.

CHAPTER 1
INTRODUCTION

## 1.1 Polymer Nanocomposites

A polymer nanocomposite is defined as an organic or inorganic phase with at least one dimension on the nanometer scale dispersed in a polymer matrix. Polymer Nanocomposites (PNC's) are used because they have shown to have enhanced material properties including improved barrier properties, tensile modulus and strength, flame resistance, abrasion resistance, and reduced shrinkage and residual strength[1]. Many industries are taking advantage of nanocomposite technologies because of recent findings regarding the low weight % of clay needed to improve properties. This makes it possible to create lightweight films and coatings for packaging with increased barrier properties. There is estimated to be a 2 order of magnitude growth of the PNC industry by the year 2005. The following are examples of a few other uses of PNC's in industry:[1,2]

- Fire Resistance – the NIST is developing fire resistant and reduced char coatings for windows and other applications.
- Asphalt Modification – Exxon is developing asphalt mixtures with improved mechanical properties using nanoparticles in mixing.
- Elastomers – many tire companies are interested in using PNC's as tire reinforcements.
- Thermoset Polymers – many industries are interested in films and coatings with improved barrier properties, abrasion resistance, and thermal stability.

Polymer nanocomposites can be isotropic or anisotropic and can have a defined structure and orientational order. Polymer nanocomposites are usually grouped into three categories based on the dimensions of the dispersed phase. Some nanoparticles are isodimensional, or have three dimensions in the nanometer range; these include all spherical, disc-shaped, or clustered particles. When there are two dimensions in the

nanoscale you can have an elongated dispersed phase such as carbon nanotubes or whiskers, which are commonly used as fillers in nanocomposites. Lastly, if there is one dimension in the nanoscale the long sheets of filler can be stacked to create a layered composite. This is achieved by the swelling of the polymer chains in between the layered sheets. Layered silicates such as Laponite are isodimensional and can be dispersed in a variety of ways.[3-5]

In layered-silicate systems, the particles can be arranged in several different structures depending on their method of preparation. When the system is phase separated, there are clumps of particles dispersed in a particle matrix with the particle and polymer phases being immiscible. In an intercalated system, the particles are arranged in layers with polymer chains swelling in between the stacked particle galleries, causing them to separate slightly. When these stacked particles are separated and dispersed throughout the polymer matrix, the system is exfoliated. The exfoliated structure is very desirable when attempting to make a well dispersed system with uniform properties. Figure 1-1 is an illustration of the different type of layered-silicate systems.[4-5]

There are several ways to prepare a polymer-layered silicate nanocomposite system to achieve intercalation or exfoliation. In situ polymerization can be used to intercalate a system by swelling the layered silicate particles in a liquid monomer and then initiate polymerization to form polymer chains between the particle sheets. In melt intercalation, if a polymer is compatible with the particle surface, the system is intercalated in the molten state during processing. An exfoliated system can also be achieved if the polymer is able to get in between the particle spacing. Layered silicates can also be exfoliated by dispersing the particles in a soluble polymer matrix where

exfoliation occurs due to delamination of the stacked particles. This is the most common method for creating an exfoliated system.[5]

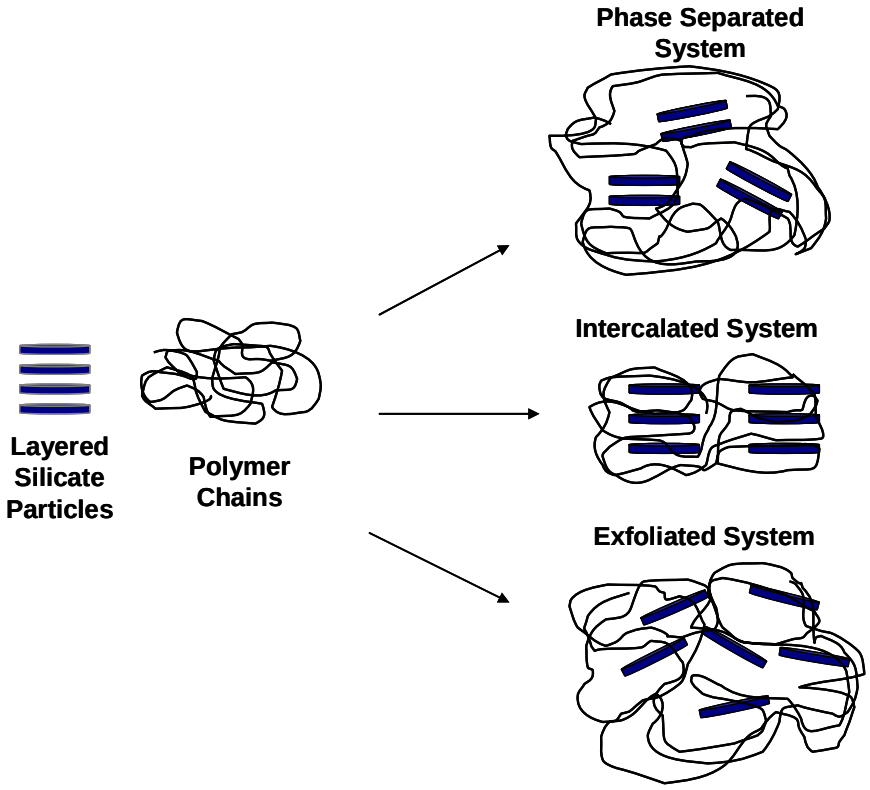


Figure 1-1: Various phases observed for polymer-layered silicate systems

In a Polyvinyl Alcohol (PVA) system containing Laponite, the particles are dispersed in the PVA matrix and a gel is formed. When the gel is dried into a film, most of the particles will become intercalated, but steric interactions in the PVA can prevent reaggragation if the molecular weight is sufficiently high.[5] The use of water-soluble polymers in these dispersions is advantageous because of environmental and safety issues which are encountered when using common organic solvents. Because of its high aspect ratio, Laponite has the ability to form a stable sol when dispersed in demineralized water at low solids loadings. When mixed with a polymer, a colloidal gel is formed.[6-12]

## 1.2 Literature Review

Numerous studies have been conducted on the nanocomposite system composed of a polymer matrix with different grades of Laponite as the dispersed phase. Most of the information available on Polymer/Laponite nanocomposites is based on the polyethylene oxide (PEO)/Laponite system. Similar to PVA, PEO is a water soluble polymer that is inexpensive and available in a wide range of molecular weights. When dispersed with surface modified Laponite particles, PEO has been shown to adsorb to the particle surface, creating bridging between the particles. When shear is applied to this mixture, the dispersion will become flocculated and a gelled network will form. These dispersions can also exhibit relaxation behavior when aged for a certain amount of time, which is dependent on the concentration of the PEO.

A recent study was done on the shear thickening and gelation of the PEO/Laponite system with applied shear.[6] In this work, the formation of a "shake-gel" was observed when a low viscosity sol composed of low concentrations of PEO and Laponite was vigorously shaken. The phase behavior of the gels, based on visual observation, is dependent on both polymer concentration and Laponite solids loading. The gelation mechanism for this system is the bridging between polymer chains when particle surfaces are exposed during the application of shear. At very high concentrations of PEO, the Laponite surface will become saturated and a gel will not form. If the PEO concentration is low, the dispersion will remain as a low-viscosity sol, so these boundaries establish a regime where a rigid gel can be formed. The authors performed light scattering experiments to determine the adsorption behavior of PEO onto the Laponite surface. Their data on the surface coverage proved to be consistent with the phase behavior that was observed.

Another study gave further insight into the network structure that can be induced by the application of shear to a PEO/Laponite system.[7] In this study, the investigators attempted to quantify the critical shear rate needed for shear-induced reorientation of the Laponite particles so that a viscous gel can be formed. The authors also studied the transitions from liquid like to gel like behavior that could be observed for these dispersions. Oscillatory shear experiments were done to find this transition, which is the point where the complex moduli intersect.

Another study examined the reversible gel behavior of the PEO/Laponite XLG system of low solids loadings.[8] Their study showed a composition regime where aggregates can be deformed by applied shear thus exposing new surface area, which leads to the formation of polymer bridges. This bridging, or flocculation, causes the gelation of the system. When shear is stopped, these polymer bridges can break up causing a relaxation in the storage modulus and reversible gel behavior. This study also determined that the reversible sol-gel transition shows time dependent characteristics.

In a study done on solid nanocomposites, dispersions of Laponite in PEO were cast onto glass substrates to form very thin films.[9] The films were cast from PEO solutions of 0, 2, and 5 weight % with a Laponite mass fraction of 3 weight %. The resulting films were observed to be transparent with good interfacial adhesion. The surface roughness and morphology of the films were characterized using Atomic Force Microscopy. The AFM images and the RMS roughness calculations showed that the particles are randomly dispersed in the film with polymer chains connecting them. The films containing low concentrations of PEO had this homogeneous structure with particles being roughly equal in size. The film cast from the 5 wt% PEO solution was observed to be heterogeneous,

with agglomerated Laponite domains separated by excess PEO. It was also observed that the roughness decreased as the PEO concentration increased because the excess polymer creates a smoother surface. The films containing low concentrations of PVA are observed to be exfoliated and randomly oriented with a high degree of surface roughness.

### 1.3 Project Background Information

Since the development of polymer nanocomposites, a wide variety of applications for these materials have been identified. Because of the improved properties that can be achieved at relatively low cost, stronger coatings and laminates can be made for military and security purposes. With the recent threats of terrorism, hurricanes, and forced entry crimes, new technologies in protective building materials have been developed. Dupont has developed several glass laminates that provide protection from these dangers using strong, transparent interlayers. For military applications involving bomb and blast protection, an abrasion resistant material is needed for protection against sharp glass shards. These small pieces of glass can become deadly projectiles when hit with a strong blast. The strong ionomer interlayers can prevent large blasts from destroying a building, but a large amount of destruction and loss of life is caused by these shards breaking off as a result of the blast. This creates a need for an adhesive, abrasion resistant coating on the polymer interlayer which will reduce or eliminate this phenomenon while maintaining the abrasion-resistance of glass. The abrasion resistant coating should be clear, flexible, and have a strong adhesion to the interlayer and the glass being used.

There are many nanocomposite systems that could be used to fabricate this coating. Laponite is a good choice for a filler phase because of its high aspect ratio and its transparency when suspended in water. Laponite particles are “water white”, which means that they are small enough to be unable to scatter light. A diagram of a single

Laponite particle is shown in figure 1-2. Surface treated Laponite particles can be mixed with a water-soluble polymer to create a stable dispersion.

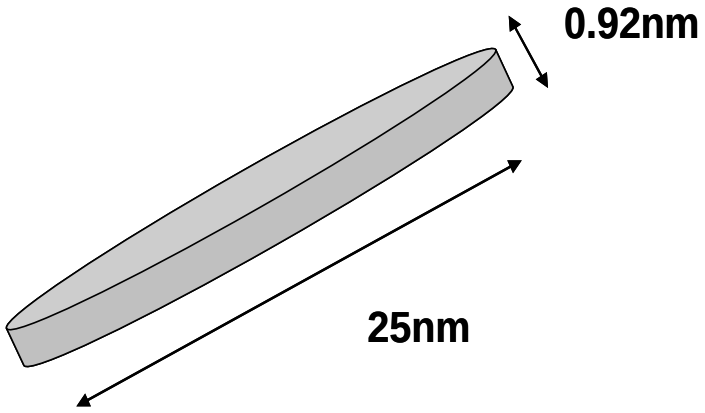


Figure 1-2: Dimensions of a Laponite particle [13]

Depending on the polymer being used, a strong, transparent film can be cast using a variety of casting methods. Polyvinyl Alcohol is known to form strong, chemical resistant films with abrasion-resistant properties. The mixture of PVA with Laponite is primarily used as a paper coating, but a system using a high molar mass PVA can form transparent films with good tensile properties.[5]

# CHAPTER 2
# RHEOLOGICAL PROPERTIES AND STRUCTURAL DEVELOPMENT

In the processing of thin, nanocomposite films, it is necessary to consider the rheological properties of the dispersions being used to cast the films. Changes in viscosity and the development of a gelled network can influence the thickness, transparency, and properties of the final film. This chapter investigates the rheological properties of various PVA/Laponite dispersions and the effect of solids loading and polymer dosage on shear viscosity and structural development.

## 2.1 Introduction

Colloidal gels are formed when a stable liquid suspension, or "sol", of colloidal particles is "gelled" using a chemical agent. In Laponite suspensions, this gelling agent is usually a filler, binder, pigment, surfactant, or wetting agent.[12,13] When Laponite particles are initially dispersed in water, sodium ions present on the dry particle surface are held between the negatively charged particles by electrostatic forces. These dispersions exhibit low-viscosity, Newtonian rheology.[13] Some Laponite grades have surface treatments that enhance the sol-forming capability of the dispersion and provide electrostatic stabilization of the sol. Laponite JS, which is used in this study, is modified with a tetrasodium pyrophosphate (TSPP) surface treatment. The $(P_2O_4)^+$ anions create a net negative charge on the particles which causes the loose layer sodium ions create repulsions between particles.[5,13] These stable sols can then be "gelled" or flocculated with the addition of a chemical agent.

Gelling agents usually come in the form of a polymer, electrolyte, or pH modifier. These compounds reduce repulsive particle-particle interactions, causing thinning of the electrical double layer present in the "sol". When the electrical double layer is sufficiently neutralized, van der Waals attractive forces draw the particles together causing a solid-like gel phase to form. The addition of polymer to a stabilized colloidal dispersion will change the properties of the dispersion depending on whether the polymer is nonadsorbing or strongly adsorbing. When a nonadsorbing polymer is added to a stable sol it can induce depletion flocculation. This occurs when two particles approach each other to a distance smaller than the radius of gyration of the polymer chain, thus the polymer is excluded from the interparticle zone. The osmotic pressure between the particles is reduced causing an attractive force to develop between particles.[12,14]

As flocculation proceeds, particle pairs (doublets) become particle triplets and so on until flocs containing many groups of particles start to appear. If the flocs are densely packed, they would form a close-packed solid structure. Instead, most flocs are open, ramified structures, or fractals, which are self-similar structures which look the same at all magnifications. As a floc grows, the porosity increases, creating a much larger, open structure. The floc can eventually grow to fill up the volume fraction of a sample, forming a percolated network, or gel.[14,15] The growth can be diffusion limited, where small flocs form to create larger flocs, or it can be reaction limited, where the density of the floc grows over time. The flocculation behavior of colloidal gels can effect the rheological behavior of the dispersion.

Understanding the rheology of gels is very important when processing these materials. Their response to shear rate, shear stress, and strain depend strongly on particle

size and shape as well as the gel strength and degree of flocculation. The rheological behavior of flocculated gels is difficult to reproduce due to their shear history and time dependent structure.[16-23] Two types of tests can be performed on colloidal gels to determine their flow properties, these are steady-shear viscosity and small amplitude oscillatory shear flow measurements. Steady shear viscosity is the most widely measured aspect of rheology and can determine whether a material is Newtonian or non-Newtonian. Using a parallel disk torsional rheometer, only a small amount of sample is needed to obtain data about the behavior of the material. Small Amplitude Oscillatory Shear (SAOS) experiments are useful in determining the viscoelastic properties of a colloidal gel. SAOS can be used to observe structural development, relaxation behavior, and various transitions for colloidal gels.[21-23]

Many rheological studies have been conducted on a colloidal system containing Laponite of different grades in a matrix of polyethylene oxide (PEO). In these systems, if the polymer concentration is not enough for full coverage, the PEO is adsorbed onto the bare surfaces of the Laponite particles and a gel forms as a result of bridging flocculation.[24] When a strong shear is applied to a PEO/Laponite suspension, the polymer chains can desorb from the particles and readsorb onto a different particle, forming a "shake gel".[6] Modulus relaxation data shows that these "shake gels" are reversible and have aging characteristics.[8]

The mixture of Laponite JS (LJS) with low molecular weight Polyvinyl Alcohol (PVA) has been used in the paper coatings industry to form coherent films with good barrier properties.[25] Relatively little is known about the rheological properties of a PVA/Laponite mixture and the effect these properties have on film processing. There are

several methods that can be used to cast the PVA/Laponite films and the rheological behavior of the dispersions determines which methods are feasible. A low-shear method would be solution casting, where the dispersion is poured over the substrate and set to dry until the solvent is evaporated. Another technique would be tape casting, which can go to very high shear rates. Some examples of shear rates at a speed of 10inches/minute are shown in Table 2-1. To obtain a very thin film, on the order of 10μm, the shear rate would be very high.

2-1: Several shear rates corresponding to common tape casting gap sizes (calculated from casting speed/gap size)

| **Gap Size** | **Shear Rate** |
|---|---|
| 3mm | 1.41 $s^{-1}$ |
| 1mm | 4.23 $s^{-1}$ |
| 0.5mm | 8.46 $s^{-1}$ |
| 0.1mm | 42.33 $s^{-1}$ |
| 0.05mm | 84.66 $s^{-1}$ |
| 0.01mm | 423.3 $s^{-1}$ |

In this study, a high molecular weight PVA is used as the matrix polymer for Laponite JS dispersions which will be used to make thin, optically clear coatings for glass and polymer substrates.

## 2.2 Materials

The polymer used in this study is a partially hydrolyzed grade of Polyvinyl Alcohol. The PVA (Aldrich Chemical Co. cat# 36310-3) has a molecular weight between 126,000-186,000 g/mol. PVA is a neutral, linear polymer synthesized from a vinyl acetate monomer with a chemical formula given by $-[CH_2 - CHOH]_n$. The PVA used in this study has a degree of hydrolysis of 87-89%, which is the extent of conversion from polyvinyl acetate to polyvinyl alcohol. The PVA is soluble in water and can easily form

thin films with good tensile strength properties on glass substrates. The films have good chemical resistance and resistance to thermal degradation.

The clay particle used in this study is Laponite (Southern Clay Products, Inc. Gonzales, TX). Laponite particles are synthetic layered nanosilicate clays with an empirical formula given by: $Na^{+0.7}[(Si_8Mg_{5.5}Li_{0.3})O_{20}(OH)_4)]^{-0.7}$.[13] The Laponite crystals are disk-shaped and are stacked when dry. The disks have a diameter of 25 nm and a width of 0.92 nm.[13] The unit cell consists of one layer of octahedral magnesium atoms with a small amount of lithium impurities. This layer is sandwiched between two layers of tetrahedral silicon atoms. Both layers are balanced by 20 oxygen atoms, 2 hydroxyl groups, and sodium ions which are released when the particles are dispersed in water.[13] Some chemical and physical properties of Laponite JS are shown in Tables 2-2 and 2-3. The grade of Laponite used for this study is Laponite JS, which is surface treated with tetrasodium pyrophosphate, an inorganic polyphosphate dispersing agent. All grades of Laponite form clear colloidal dispersions when mixed with water.

2-2: Chemical composition of Laponite nanoparticles[13]

| **Material** | **Weight %** |
|---|---|
| $SiO_2$ | 50.2 |
| MgO | 22.2 |
| $Li_2O$ | 1.2 |
| $Na_2O$ | 7.5 |
| $P_sO_5$ | 5.4 |
| F | 4.8 |

2-3: Physical properties of Laponite nanoparticles[13]

| **Property** | **Value** |
|---|---|
| Appearance | Free flowing white powder |
| Bulk Density | 950 kg/m$^3$ |
| Surface Area (BET) | 300 m$^2$/g |
| Loss on ignition | 8.70% |
| pH (2% suspension) | 10 |
| Storage | Hygroscopic, should be stored under dry conditions |

## 2.3 Experimental Procedure

### 2.3.1 Sample Preparation

The polymer stock solutions are made by dissolving PVA granules in deionized water at room temperature and stirring at moderate speeds for 24 hours with a magnetic mixer. The Laponite dispersions are made by mixing 200 mL of polymer stock solution with a given amount of Laponite (according to final solids loading in films) at pH 10. These dispersions are mixed with a high shear mixer (Hamilton Beach Commercial Shear Mixer 950) to ensure good mixing and prevent aggregation. Defoaming agents are used when needed to prevent viscous bubbles from forming, which can alter the rheological results and weaken the final films. The polymer/clay dispersions are agitated on a shaker for 48 hours prior to rheological measurement to ensure good mixing. The samples were kept mixing until they were measured to avoid effects of time dependency, which is common for polymer/Laponite dispersions.[6-8]

The nanocomposite film samples were made by solution casting the PVA/Laponite gel dispersions onto glass petri dishes at 35°C. They were left to evaporate in a convection oven for 24 hours, or until they were observed to be completely dry. The

film quality is improved by this slow evaporation process since the clay platelets have more time to assemble under gravitational and osmotic forces[16]. These nanocomposite films are optically clear with the Laponite phase trapped in the thin film resulting in good interfacial adhesion to the glass substrate.[9]

**2.3.2 Rheological Measurements**

A Paar Physica UDS 200 Rheometer was used to examine the steady- and oscillatory-shear-flow using a parallel plate geometry (plate radius, 2.5cm). Steady shear flow experiments were conducted to determine steady shear viscosity (η) as a function of shear rate ( $\dot{\gamma}$ ) with shear rates ranging from 1-5000 $s^{-1}$. Oscillatory shear flow experiments were performed to determine the viscoelastic properties of the dispersions. The storage (G′) and loss (G″) moduli are related to the real and imaginary components of the complex viscosity, η′ and η″ respectively. With a given angular frequency (ω) and phase shift (δ) they can be calculated as follows:

$$\tan\delta = \frac{G'}{G''} \qquad 2.1$$

$$\eta' = \frac{G'}{\omega} \qquad 2.2$$

$$\eta'' = \frac{G''}{\omega} \qquad 2.3$$

And finally, the complex moduli can be related to the complex viscosity by

$$\eta^* = \eta' - i\eta'' = G^* = \frac{G''}{\omega} - i\frac{G'}{\omega} \qquad 2.4$$

Where $i = \sqrt{-1}$ . An angular frequency range of 1-50 Hz was chosen with a fixed strain amplitude of 5% to maintain the measurements in the linear viscoelastic region.[26-28] Sample evaporation is prevented by using a circular solvent trap covered with an

aluminum cap, which isolates the sample during measurement. All experiments were performed at a temperature of 25°C.

There are several sources of error that must be considered when performing rheological measurements. Factors such as humidity, sample size, and ambient temperature can have an effect on the sample behavior. For the following experiments, each batch of samples had one repeat for every three samples run. This repeat was compared to the original data to verify the reproducibility of the experiment within +/- 3%. Since Laponite dispersions are known to have a time-dependency,[8] all samples were kept on a shaker until use.

**2.3.3 Microscopy**

Scanning Electron Microscopy (SEM) was done on the films to determine the structure of the laponite particles in the cast films. Images were taken using a JEOL JSM-6335F Scanning Electron Microscope to examine the structure inside a solution cast nanocomposite film with a final solids loading of 50 wt% from a Laponite dispersion prepared in a 3% PVA matrix. The film sample was mounted onto an aluminum mount and coated with Gold-Palladium to improve conductivity. The image was taken at a 2000x magnification and a beam energy of 1kv to prevent destruction to the polymer matrix of the film.

Atomic Force Microscopy (AFM) was performed to examine the surface morphology of the nanocomposite films. The films used for AFM were also cast from a 3 wt% PVA matrix with Laponite solids loading of 0, 40, 50, and 60 wt%. The measurements were done at a setpoint of 2 volts, a scan rate of 3 Hz, and a scan size of 1 μm.

## 2.4 Discussion of Results

### 2.4.1 Shear Viscosity

**2.4.1.1 Effect of shear rate on viscosity.** The steady shear viscosity (η) as a function of shear rate ($\dot{\gamma}$) was measured in three dispersion systems, one which varied polymer dosage, one which looked at final solids loading in cast films, and one system which varied Laponite solids loading. The effect of shear rate on the steady shear viscosity of dispersions containing Laponite nanoparticles dispersed in solutions of PVA at dosages ranging from 1 to 12 mg/(g solids) and a Laponite loading of 10 wt% is shown in Figure 2-1. It can be observed at low polymer dosages the Laponite can form a stable sol which exhibits a constant viscosity ($\eta_o$) and Newtonian behavior in the shear rate range examined. At high polymer dosages, the viscosity of the dispersions decrease with increasing shear rate, i.e., they exhibit shear thinning, or thixotropic, behavior at high shear rates. These data show that with increasing polymer dosage there is almost four degrees of magnitude increase in viscosity, which can be seen for dosages above 3mg/(g solids). As polymer is added to the Laponite dispersions, they swell between the particles and cause an increase in the zero shear viscosity. With an increase in applied shear rate, the particles and polymer chains align themselves in a more desirable flow structure, causing shear thinning in the system.

The Laponite solids loadings used in Figure 2-2 are the actual concentrations of filler that would be used to process nanocomposite films with final solids loadings of 40 wt%, 50 wt%, and 60 wt%. These samples were prepared in a 2 wt% PVA solution as the suspending media and are high enough to produce films of good tensile strength. The characteristics of these films are shown in Table 1. The data in Figure 2 shows the relationship between shear viscosity and shear rate for several calculated Laponite solids

loadings in 2 wt% PVA solution. The dispersions containing very low weight fractions of Laponite maintain a constant viscosity ($\eta_o$) and behave as Newtonian fluids throughout the range examined. The further addition of Laponite causes an increase in the zero shear viscosity ($\eta_o$) and the onset of shear thinning shifts to lower shear rates.

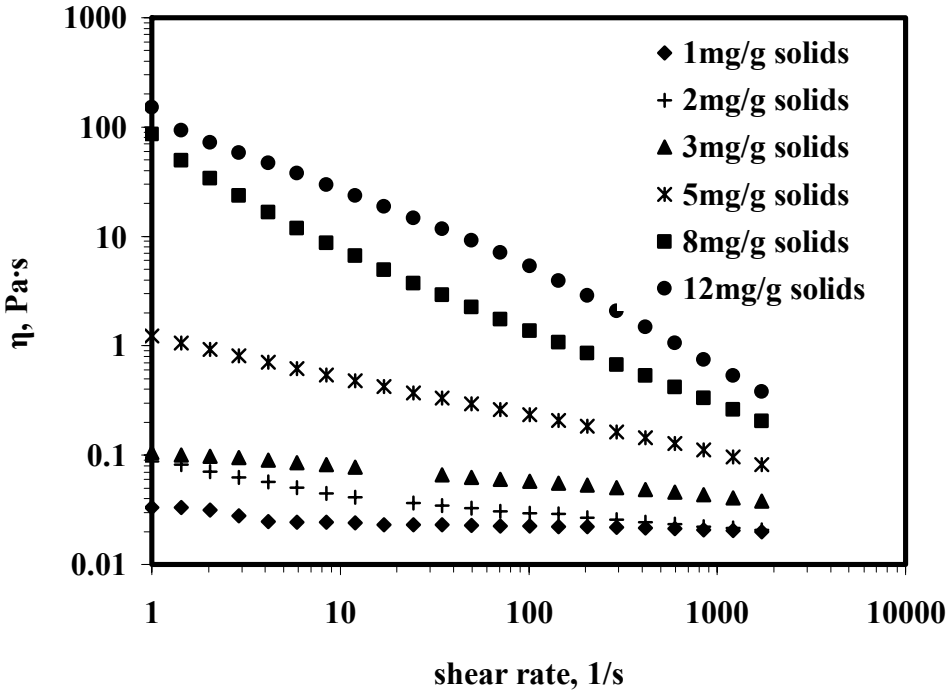


Figure 2-1: Viscosity as a function of shear rate for dispersions of 10wt% Laponite with increasing polymer dosages (25°C).

Table 2-4: PVA/Laponite dispersion and film characteristics

| Wt% PVA in water | PVA Mass Fraction in dried films | Mass fraction Laponite in Solution ( wt%) | Laponite mass fraction in dried films |
|---|---|---|---|
| 2% | 60% | 1.3 | 40% |
| 2% | 50% | 1.96 | 50% |
| 2% | 40% | 2.91 | 60% |
| 3% | 60% | 1.96 | 40% |
| 3% | 50% | 2.91 | 50% |
| 3% | 40% | 4.3 | 60% |

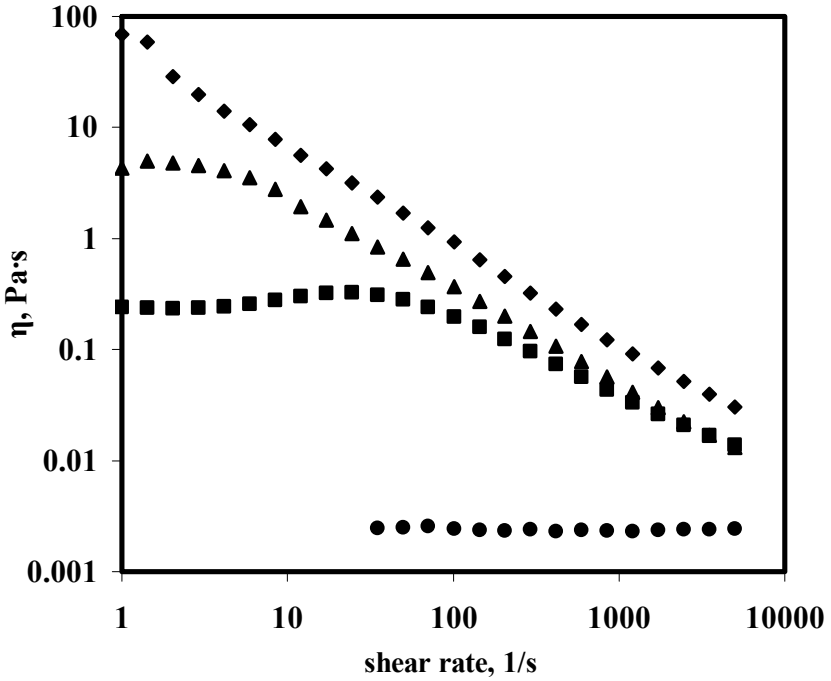


Figure 2-2: Viscosity as a function of shear rate for dispersions of Laponite JS in 2 wt% PVA solution (25°C) at different wt% solids: (●) 0 wt% (■) 1.3 wt% (▲) 1.96 wt% (♦) 2.91 wt%.

The shear viscosity data are shown in Figure 2-3 for dispersions of Laponite particles at solids loadings ranging from 0-5 wt% prepared in a 1 wt% PVA stock solution. The viscosity shows changes with both shear rate and volume fraction of the particles. At a fixed weight fraction and at low shear rates, all samples show Newtonian behavior. For these low weight fractions, lower shear rates are not in the linear range of the instrument, and are therefore left out of the data. At moderate shear rates, the viscosity falls monotonically with increasing shear rate and there is no indication of a second plateau at high shear rates. There is at least three orders of magnitude change of viscosity as the solids loading is increased. A transition from a shear rate independent region (Newtonian plateau) to a shear rate dependent region occurs at low shear rates as the solids loading is increased. Over the shear rate dependent region, the plots of

viscosity as a function of shear rate are approximately linear. Therefore, the linear region of the plots of log η as a function of log $\dot{\gamma}$ can be described by the power law model.

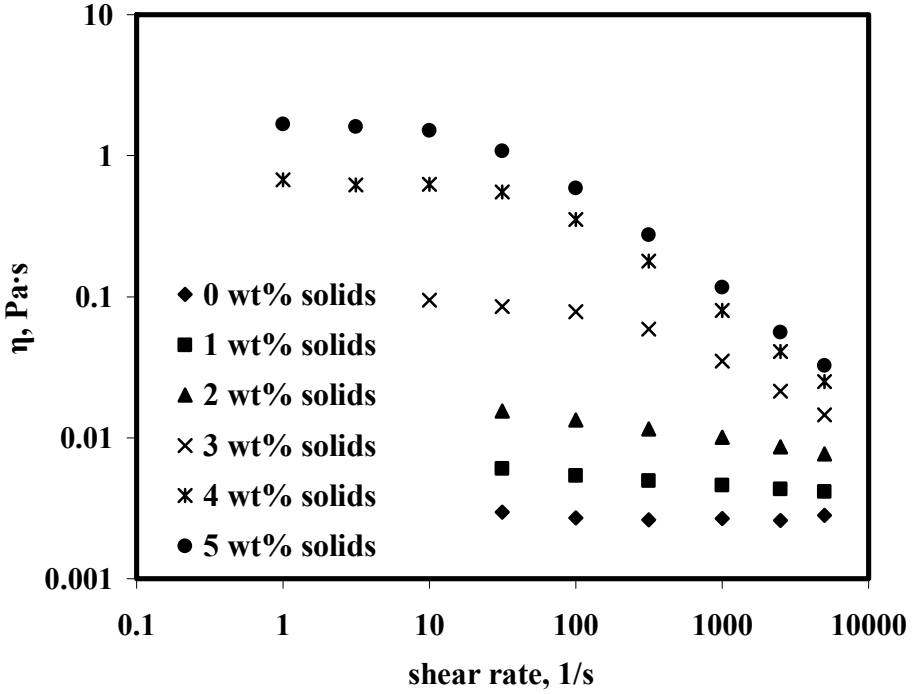


Figure 2-3: Shear viscosity as a function of shear rate and solids loading for dispersions made from 1 wt% PVA Solution (25°C).

Figure 2-4 represents the shear viscosity data for dispersions of Laponite particles of 4 wt% solids loading dispersed in solutions of 1 wt% PVA and 3 wt% PVA solutions respectively. It can be observed that the dispersion containing 3 wt% PVA has a viscosity that is one degree of magnitude larger than that for the 1 wt% PVA. Both show Newtonian behavior at low shear rates and shear thinning behavior at high shear rates. Additionally, the onset of shear thinning occurs at the same shear rate for both curves.

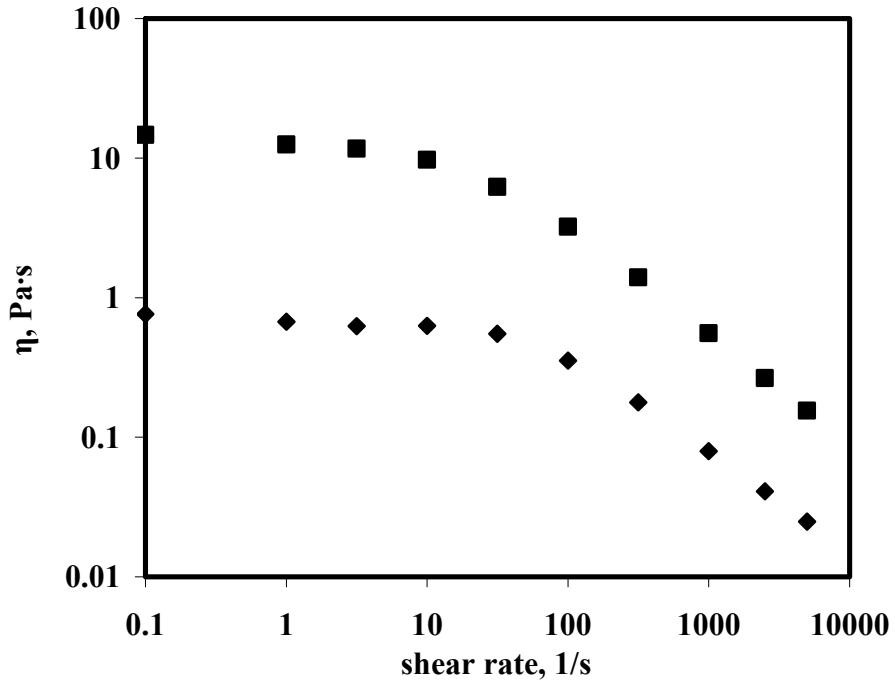


Figure 2-4: Viscosity as a function of shear rate for dispersions of 4 wt% Laponite prepared in 1 wt% PVA and 3 wt% PVA solutions (25°C) (♦) 1 wt% PVA (■) 3 wt% PVA.

The relative viscosity data as a function of shear rate for the above mentioned dispersion are presented in Figure 2-5. The viscosity data are normalized with respect to the viscosity of 1 wt% and 3 wt% PVA solutions as the suspending media. There is not a significant difference in the relative shear viscosities of the two dispersions. This behavior indicates that increase in the viscosity is solely due to increase in the viscosity of the suspending media with PVA concentration. Since the shape of the curves stays the same when the effect of the polymer is removed, it may be that polymer-particles interactions in the polymer/clay dispersions are not dominating the rheological behavior of the system.

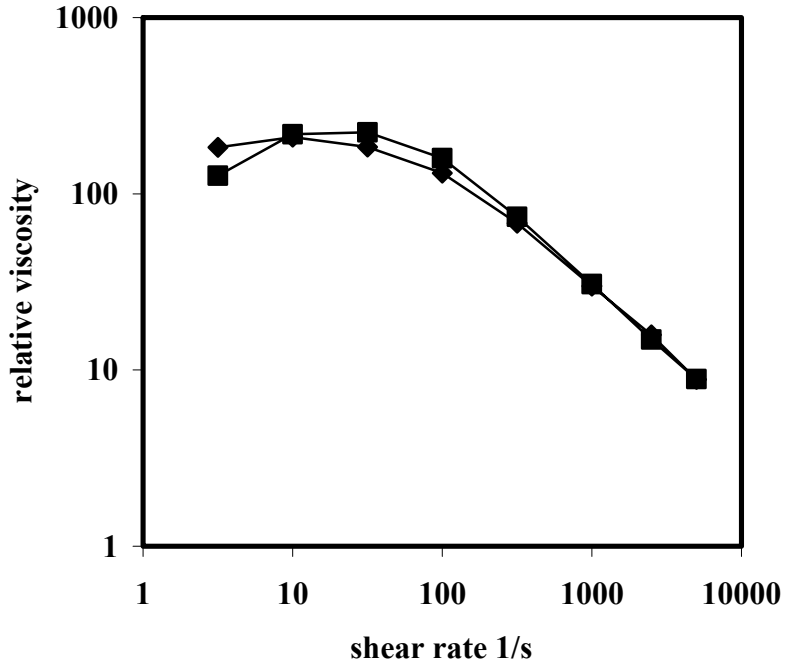


Figure 2-5: Relative viscosity (with respect to the viscosity of the suspending fluid) as a function of Shear rate for dispersions of 4 wt% wt Laponite dispersions prepared in 1 wt% PVA and 3 wt% PVA solutions (25°C) (♦) 1 wt% PVA (■) 3 wt% PVA.

**2.4.1.2 Effect of solids loading on viscosity.** As with most general polymer/filler systems, it appears that the differences in viscosity at various volume fractions are more significant at low shear rates. The viscosity as a function of solids loading at shear rates of 1 $s^{-1}$ and 1000 $s^{-1}$ for dispersions prepared in 1 wt% PVA solutions is shown in Figure 2-6 and can be observed at low shear rates. Addition of the Laponite filler can cause the viscosity to increase by an order of magnitude. At low shear rate, the viscosity of the system is dominated by particle-particle, polymer-particle, and structure of the dispersions. While at high shear rates, hydrodynamic forces are dominant and control the viscosity of the system. From a processing point of view, it is more convenient to process these materials at higher shear rates due to the significant decrease in viscosity at higher

shear rates. At low shear rates, processing would be very slow and can result in defects such as bubbles and cloudy spots in the final product.

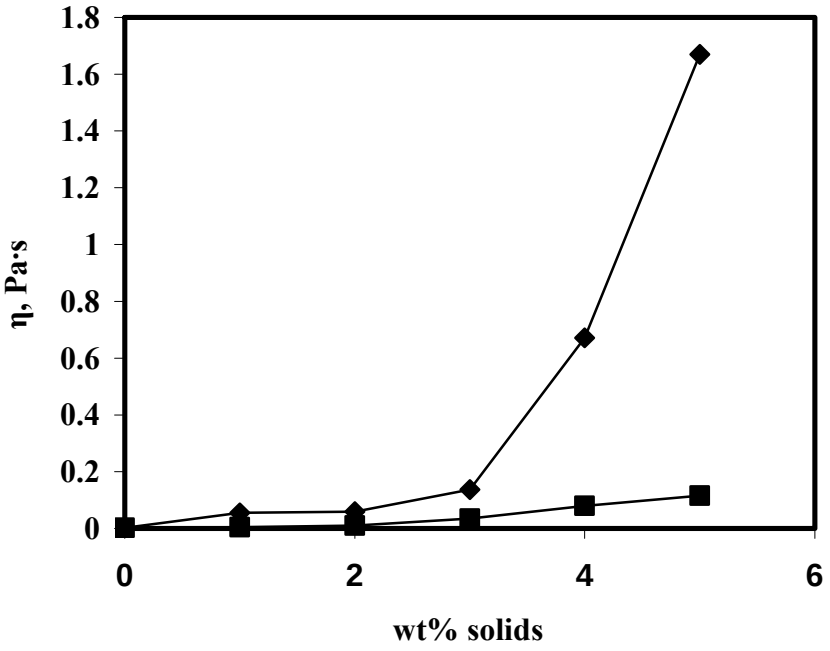


Figure 2-6: Viscosity as a function of solids loading for dispersions of Laponite particles prepared in a 1 wt% PVA solution at two different shear rates (♦) 1 $s^{-1}$ (■) 1000 $s^{-1}$.

### 2.4.2 Viscoelastic Properties and Structural Development

The effect of polymer dosage on the structural development of the colloidal gels can be determined using small amplitude oscillatory shear measurements at different dosages. The response of the dispersions, at 10 wt% Laponite, to small-amplitude oscillatory-shear flow is shown in Figure 2-7. At the lowest polymer dosage (1mg/(g solids)), a low storage modulus can be observed, suggesting that at this concentration, the dispersion behaves as a viscoelastic liquid, unable to store large amounts of elastic energy. In the range of 2-5mg/(g solids), there is a structural transition between liquid and solid behavior where the value of the storage modulus drops, indicating a breakdown

in the flocculated viscoelastic gel structure. At polymer dosages above 5mg/(g solids), there is a very weak frequency dependence of the storage modulus, so the viscoelastic gel does not break down at high frequencies. This transitional behavior of the dispersions at moderate polymer dosages suggests a dependence of the structural breakdown of the gel on the polymer concentration used. The higher the polymer concentration, the less likely it is for a breakdown from solid-like behavior to liquid-like behavior to occur. The interactions between polymer and particles contribute to the elastic properties of the dispersions, especially since the dispersions are initially flocculated. At the frequencies where the breakdowns are occurring, the weakly bonded percolated network structure is breaking down.

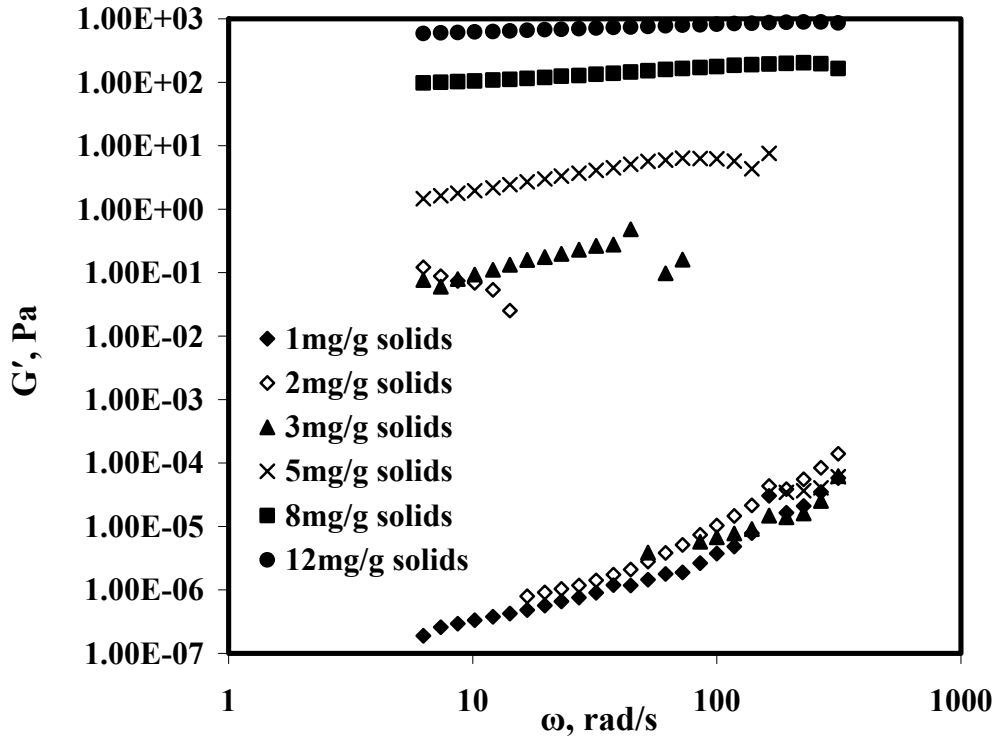


Figure 2-7: Storage modulus vs. angular frequency and polymer dosage for dispersions of 10 wt% Laponite particles (25°C).

A comparison for the storage modulus data as a function of angular frequency for dispersions of Laponite (at calculated solids loadings) in 2 wt% and 3 wt% PVA matrices are shown in Figures 2-8 and 2-9. In both plots, the dispersions containing no Laponite show liquid-like behavior throughout the range examined. For the 2 wt% dispersions, there is a breakdown of the gel structure from solid-like behavior to liquid-like behavior at high frequencies for all Laponite. This occurs for all three Laponite solids loadings, although the onset of liquid-like behavior shifts to high frequencies as the solids loading is increased. For the 3 wt% PVA dispersions, the storage modulus has a weak dependence on frequency and stays relatively constant through the range shown, increasing slightly as the frequency is increased.

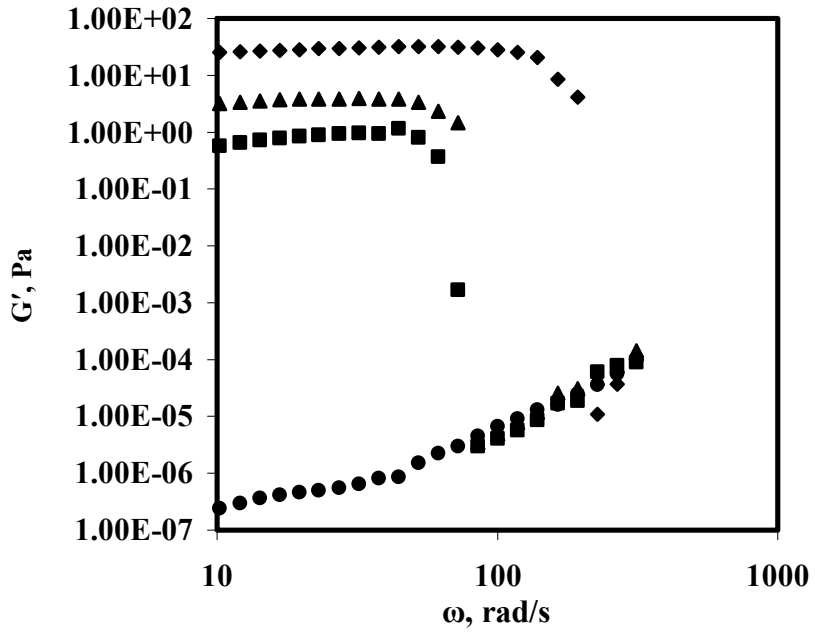


Figure 2-8: Storage modulus as a function of angular frequency for dispersions of Laponite prepared in 2 wt% PVA solution (25°C) (●) 0 wt% (■) 1.3 wt% (▲) 1.96 wt% (♦) 2.91 wt%.

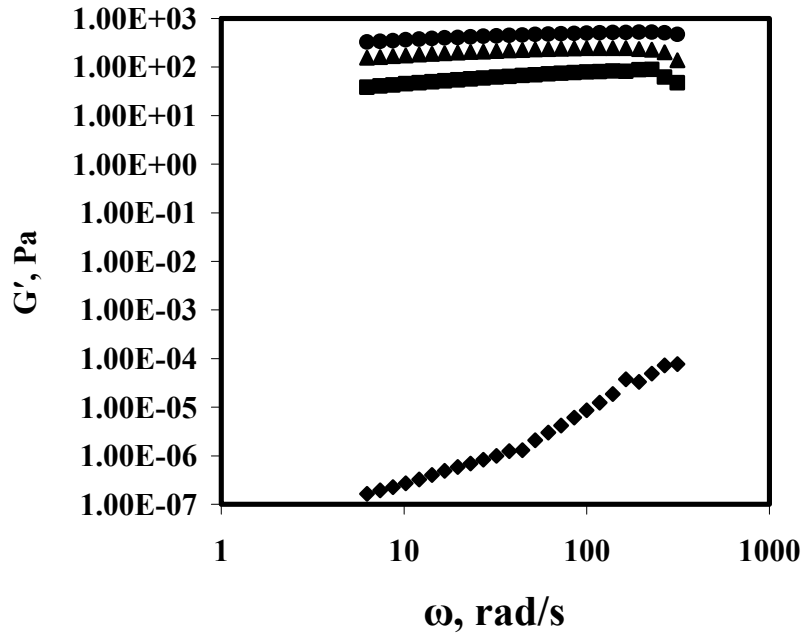


Figure 2-9: Storage modulus as a function of angular frequency for dispersions of Laponite particles prepared in 3 wt% PVA solution (25°C) (♦) 0 wt% (■) 1.96 wt% (▲) 2.91 wt% (●) 4.3 wt%.

The corresponding loss modulus data for the 2 wt% and 3 wt% PVA samples are shown in Figures 2-10 and 2-11. At both PVA concentrations, the samples containing no Laponite have a steady increase in loss modulus as the angular frequency is increased. Comparing these with the storage modulus data, the value of loss modulus is consistently higher than that of the storage modulus, suggesting that the dispersions containing no Laponite exhibit liquid-like behavior for all frequencies. For the 2 wt% PVA dispersions containing Laponite, the loss modulus stays steady at low frequencies with the magnitude of the storage modulus being larger than that of the loss modulus, showing solid-like behavior. At higher frequencies, there is a sharp increase in loss modulus, and the dispersions go from solid-like behavior, to liquid-like behavior. This phenomenon is not observed for the 3 wt% PVA dispersions because of the increase in polymer

concentration. As the angular frequency is increased, the loss modulus stays constant at a value below the storage modulus, showing solid-like behavior for all angular frequencies.

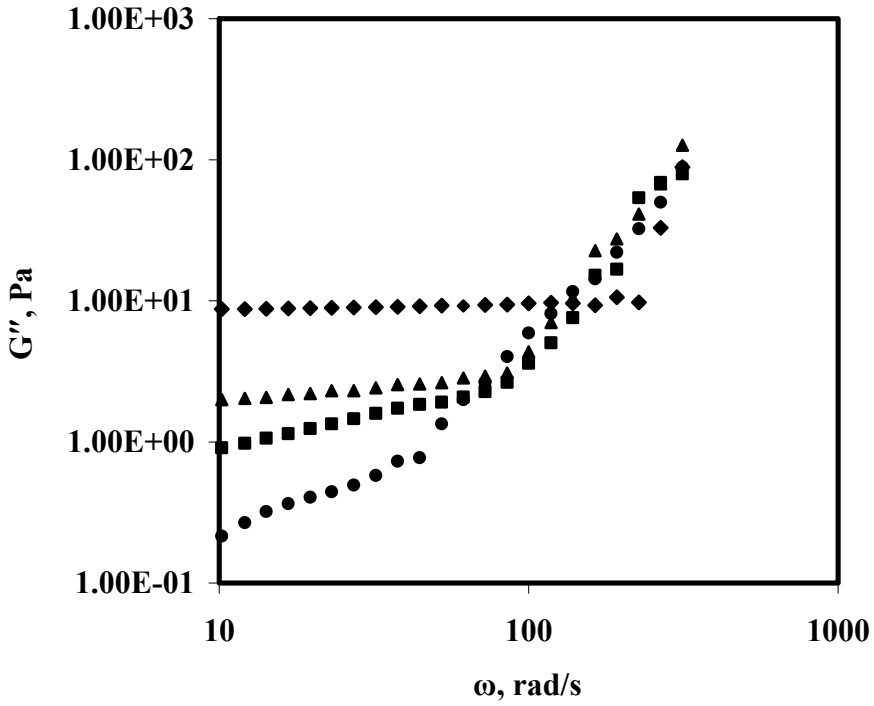


Figure 2-10: Loss modulus as a function of angular frequency for dispersions of Laponite particles prepared in 2 wt% PVA solution (25°C) (●) 0 wt% (■) 1.3 wt% (▲) 1.96 wt% (♦) 2.91 wt%.

### 2.4.3 Microscopy

Figure 2-12 is a scanning electron microscope image depicting the fractal structure of the Laponite nanoparticles dispersed in a polymer matrix. This floc appears to be 30-40μm in diameter, and is frozen in the film. The floc is not connected with other flocs in the vicinity. It is apparent from this image that this is not a percolated networked structure, which is formed when a fractal network grows to create an interconnected three-dimensional network structure. The formation of the fractal network in these films may be due to aggregation over long time scales.[15]

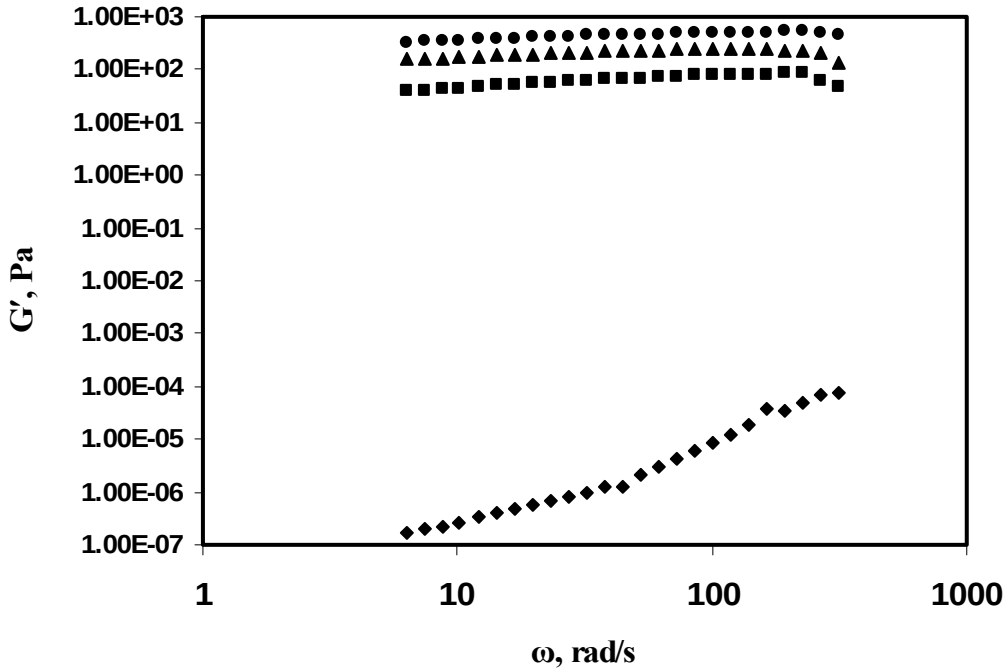


Figure 2-11: Loss modulus as a function of frequency for dispersions of Laponite particles prepared in 3 wt% PVA Solution (25°C) (●) 0 wt% (■) 1.3 wt% (▲) 1.96 wt% (♦) 2.91 wt%.

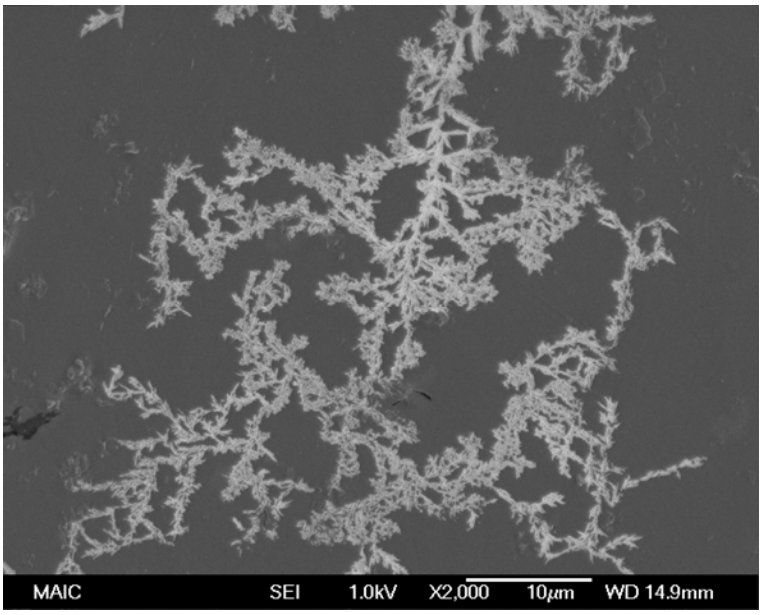


Figure 2-12: SEM micrograph of flocculated Laponite particles cast from a 3 wt% PVA dispersions with 50 wt% Laponite mass fraction in dried film.

The freely dispersed flocs present in the SEM image of the PVA/Laponite system interact through non-covalent bonds such as van der Waals attractive forces and hydrostatic interactions. Under high shear rate or a high frequency, the weakly bonded gel can breakdown, creating a discontinuity in solid-like behavior, as previously discussed. The dimensions and density of the fractal structures have an effect on the properties of the dispersions and the cast films. These properties can be determined using computational modeling and mathematical analysis.[24]

Atomic force microscope images for several different film solids loadings are shown in Figure 2-13. These pictures show that the clay particles are randomly oriented in the film and are connected by polymer.[9] A film containing no laponite is shown in Figure 2-13A, this image shows a smooth surface with some variation in height but a very small roughness. The images of the films containing Laponite particles show surfaces with some roughness and many height variations due to particles at the surface. The 40 wt% film has some where the height decreases, suggesting that the polymer matrix exists between the particles. As the solids loading is increased, there are less areas where the polymer exists and the height increases, which may due to particles aggregating on film surface.

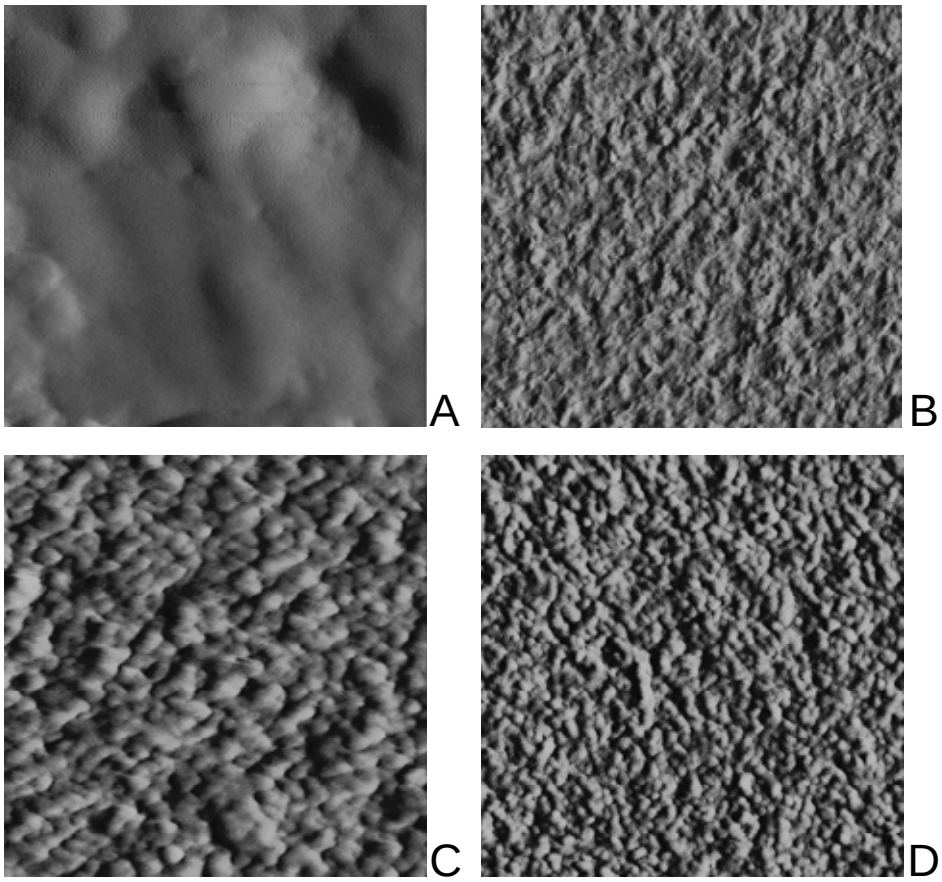


Figure 2-13: AFM images of dry films cast from a 3 wt% PVA matrix with final solids loadings of A.) 0 wt% B.) 40 wt% C.) 50 wt% D.) 60 wt%.

# CHAPTER 3
# SURFACE ACTIVATION

## 3.1 Introduction

In order to adhere polymer nanocomposite films onto a polymer substrate, there needs to be good interfacial adhesion between the two materials. Many polymer substrates are hydrophobic, or have a high surface tension, and it is difficult to adhere a water-based film to that type of surface. To form a bond between the film and the substrate, the surface tension must be reduced and the surface of the substrate must be activated so that covalent bonds can form between the film and the surface.[29]

There are several ways to activate the surface of a material to create functional groups capable of improving interfacial adhesion. These methods include wet-chemical treatments, mechanical treatment, exposure to flames, ultraviolet radiation, and ion beams.[29-33] Plasma treatment is considered the most efficient way to activate a polymer surface for adhesion to metal.[29] This technique can provide surface activation without effecting the bulk properties of the material. In a gas plasma process, weak bonds on the surface of a material are replaced by highly reactive carboxyl, carbonyl, and hydroxyl groups. This is achieved by exposing the surface of a material to ionized gas containing ions, atoms, electrons and neutral species; this process is done in a vacuum.[30] Although there are many advantages to this process, it requires expensive equipment. The most cost effective way to create surface chemical functionalization is by using various wet-chemical treatments. These treatments work by removing a weak surface boundary layer

from the polymer interface, creating covalent bonds at the surface. Some common materials used for these treatments include various acids and coupling agents. When exposed to a polymer surface, these chemicals will change the composition of the surface, creating active domains capable of bonding with a hydrophilic interface.[32]

In order to determine the success of a surface treatment, the chemical composition of the surface must be analyzed before and after the treatment. Fourier Transform Infrared (FTIR) spectrometry is ideal for evaluating changes on the surface of a material. Using Attenuated Total Reflectance (ATR), a sampling of the material surface can be taken with little sample preparation compared to traditional transmission sampling.[30,32] For this method, a total internally reflecting IR beam will come in contact with a dense crystal with a high refractive index at a certain angle. When the sample is in direct contact with the infrared beam it will be absorbed by an IR absorbing material sample. The adsorption wave will be attenuated in the sample and the data will be sent to a detector and an infrared spectrum will be generated. A schematic of the mechanism of an ATR sampling is shown in Figure 3-1. Sample spectra collected using ATR are different from those obtained by transmission. Shifts in band intensity and frequency can result in displacements of peak maximums and intensity.[30] Because of these differences, it is difficult to perform quantitative analysis using ATR.

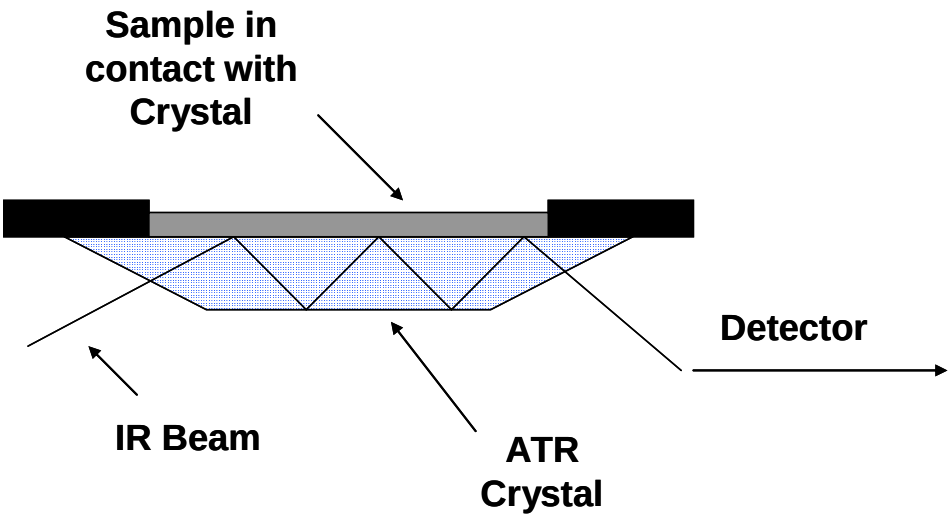


Figure 3-1: Schematic of Attenuated Total Reflection (ATR)[30]

### 3.2 Materials

A SentryGlas® Plus Ionomer Interlayer was obtained from the Air Force and was manufactured by Dupont. It is composed of an ethylene/Methacrylic Acid copolymer with trace amounts of sodium salts. The material is non-toxic and stable at normal temperatures. Some of the typical properties of the interlayer are shown in Table 3-1.

3-1: Characteristics of Dupont SentryGlas® Plus ionomer interlayer

| Characteristics | Metric Unit | Metric Value | Test |
|---|---|---|---|
| Young's Modulus | MPa | 300 | ASTM D-5026 |
| Tear Strength | MJ/m3 | 50 | ASTM D-638 |
| Tensile Strength | MPa | 34.5 | ASTM D-638 |
| Elongation | % | 400 | ASTM D-638 |
| Density | g/cm3 | 0.95 | ASTM D-790 |
| Flex. Modulus (73°F) | MPa | 345 | ASTM D-790 |
| Coefficient of Expansion (-20°C to 32°C) | 10-5 cm/cm C | 15-Oct | ASTM D-696 |

The acids used for the surface treatments were sulfuric acid (Fisher Scientific) and nitric acid (Fisher Scientific). Several different silane coupling agents were used for surface treatments. The silanes used in this study are listed below:

- 2 – (3,4 – Epoxycyclohexyl) Etheltriethyl Triethoxysilane
- 5,6 Epoxyhexyltriethoxysilane
- 11 – (Triethoxysilyl)udecanal
- 3 – Aminopropyl Trimethoxysilane
- N – (2 – Aminoethyl) – 3 – Aminopropyl Trimethoxysilane
- N – (2 – Aminoethyl) – 3 – Aminopropylsilanetriol 25%
- Bis (2 – Hydroxyethyl) – 3 – Aminopropyl Triethoxysilane, 62% in ethanol
- Vinyl terminated PDMS - fumed silica reinforced
- Pentamethyl cyclopentasiloxane

Some of these silane coupling agents turned the interlayer samples yellow, so not all of them were used as film substrates.

## 3.3 Experimental Procedure

### 3.3.1 Sample Preparation

Two different chemical treatments were used to activate the surface of the interlayer samples, acid treatments and silane coupling agents. The acid treatment was used to oxidize the surface by varying the concentration of a mixture sulfuric and nitric acid. Treatments containing no nitric acid were also used, but the sulfuric acid was diluted to different levels. For these treatments, the interlayer sheets were thoroughly cleaned with deionized water and cut into 1.5 inch by 3 inch rectangular coupons using a shear cutter. The acid solutions were mixed on a magnetic stir plate and allowed to equilibrate to room temperature. The interlayer coupons were dipped into the acid solutions for two minutes using Teflon-coated tweezers. After being removed from the solution, the treated samples were dipped in water to clean off any excess acid solution

and dried with a towel. This method was used for all acid-treated samples at all concentrations.

For the silane coupling agent treatments, a 1ml transfer pipette was used to drop the coupling agent onto the surface of the interlayer coupons. All samples were treated for one minute and then washed with deionized water until all excess coupling agent was removed from the surface. Any samples that instantly yellowed on contact with the silane coupling agent were disqualified as surface modifiers and were no longer used in the experiment.

Nanocomposite films were cast onto the treated interlayer substrates by solution casting in a convection oven at 25°C. The interlayer coupons were put into plastic Petri dishes and 75mL of the dispersions were poured into the dish to cover the interlayer samples. Dispersions in 1, 2, and 3 wt% polymer matrices were prepared with solids loadings corresponding to dry film concentrations of 40, 50, and 60 wt% for each polymer solution.

### 3.3.2 Fourier Transform Infrared Spectroscopy (FTIR)

The FTIR experiments were performed using a Nicolet MAGNA 760 Bench with Spectra Tech Continuμm IR Microscope. The samples were analyzed using the IR Microscope with an ATR objective slide-on microscope accessory. A silica crystal with a refractive index of 3.4 was used to analyze the sample by contact with the surface. The microscope assembly was cooled with liquid nitrogen before using the microscope and ambient gases were pumped into the IR chamber. The samples were loaded onto the microscope platform, surface treated side facing the crystal. Before the sample comes in contact with the crystal, a background spectra is taken to assess the amount of noise in the instrument before sampling. The microscope is then pressed onto the sample surface

until the Contact Alert™ system signaled the position where optimal contact pressure is achieved for repeatable results. A set number of samples are taken until a smooth curve is produced. The single beam spectra from the background and then again from the sample are combined and a total absorbance is determined using the following formula:[30]

$$\log(\frac{1}{R}) = -\log(\frac{sample}{Background}) \qquad 3\text{-}1$$

This is also related to sample reflectance (r) by

$$\log(\frac{1}{R}) = -\log(r) \qquad 3\text{-}2$$

The magnitude of log(1/R) is also proportional to the concentration of bonds on a sample surface, which is useful in performing qualitative analysis on the change of a sample surface.

## 3.4 Discussion of Results

### 3.4.1 Acid Surface Treatments

There were several different acid treatments applied to the interlayer samples to produce a change in the surface properties. The FTIR provided information about changes in the chemical structure of the interlayer surfaces. Figure 3-2 is an FTIR curve for the untreated interlayer specimen. The largest peaks in the spectrum correspond to two very large $CH_2$ peaks at 2917 $cm^{-1}$ and 2850 $cm^{-1}$. There are also several smaller peaks that also correspond to C-H and $CH_2$ bonds in polyethylene, some of these peaks are represented in Table 3-2 from information obtained on the OMNIC software. The spectral libraries in the ONMIC software matched the curves with that of low density polyethylene, which is consistent with the polyethylene matrix of the interlayer material. The second phase of the interlayer copolymer, methacrylic acid, was not observed in the

spectral libraries. This spectrum was reproducible when moved to different sections of the sample and when analyzed several times at one spot.

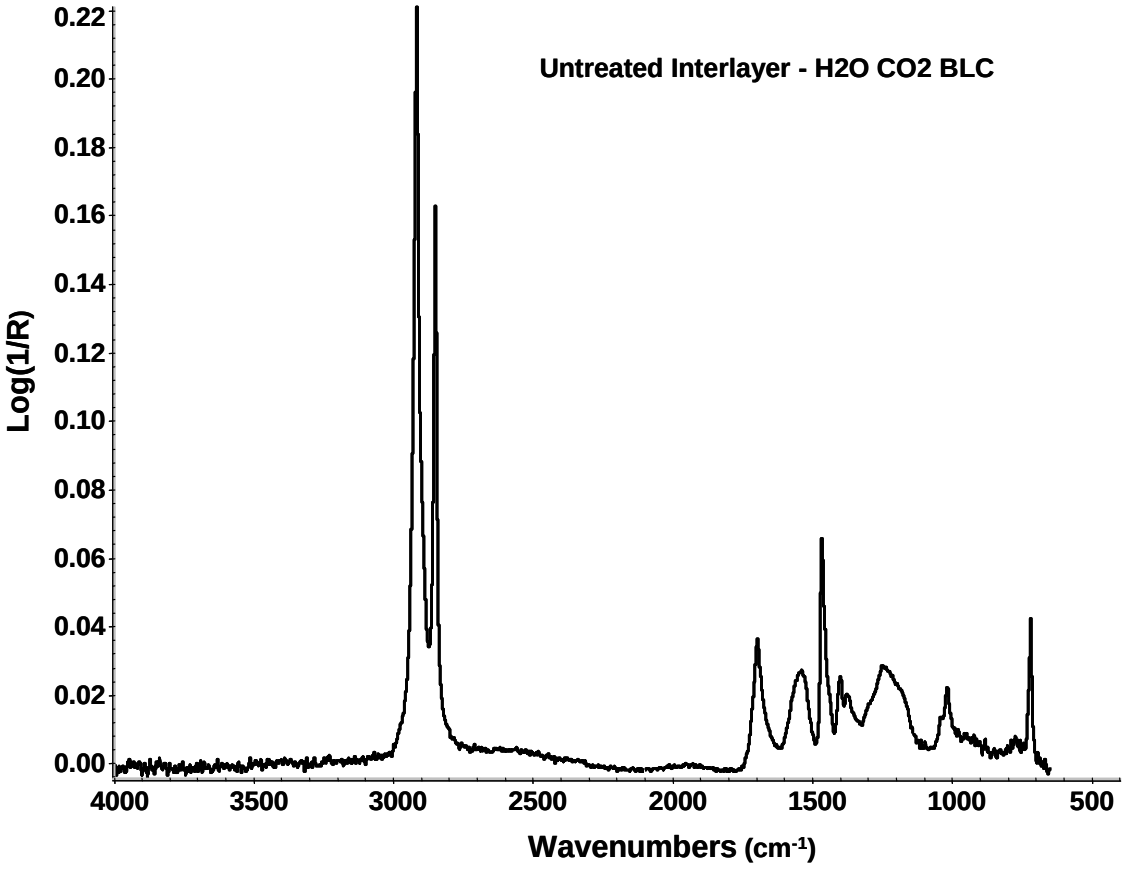


Figure 3-2: Infrared spectrum for the surface of an untreated interlayer sample**.**

Table 3-2: Absorption frequencies for common bonds found in OMNIC software.

| **Bond** | **Assignment** | **frequency range $cm^{-1}$** |
|---|---|---|
| CH, $CH_2$, $CH_3$ | Stretching | 2850-3000 |
| CH | bend | 675-1000 and 1350-1470 |
| $CH_2$ | wag | 1450-1470 |
| C=O | stretch | 1650-1870 |
| Si-OR | stretch | 1000-1100 |
| Si-H silane | stretch | 2100-2360 |

The FTIR plot in Figure 3-3 is for an interlayer sample treated with a 100% concentrated solution of sulfuric acid. This highly concentrated solution caused some yellowing on the surface of the interlayer, but a change in the surface chemistry is observed. The two $CH_2$ peaks are still present in the spectrum, but a new large peak is observed at a wavelength of approximately 1150 $cm^{-1}$, which corresponds to a carbonyl (C=O) stretch bond frequency. Using the spectral libraries on the OMNIC software, this value corresponds to an acid group on the surface of the interlayer. It can also be observed that the height of the $CH_2$ peaks at 2917 $cm^{-1}$ and 2850 $cm^{-1}$ is less that that observed for the untreated interlayer. This occurs because the new activated groups on the surface of the interlayer increased in concentration, so the amount of polyethylene observed on the surface will decrease.

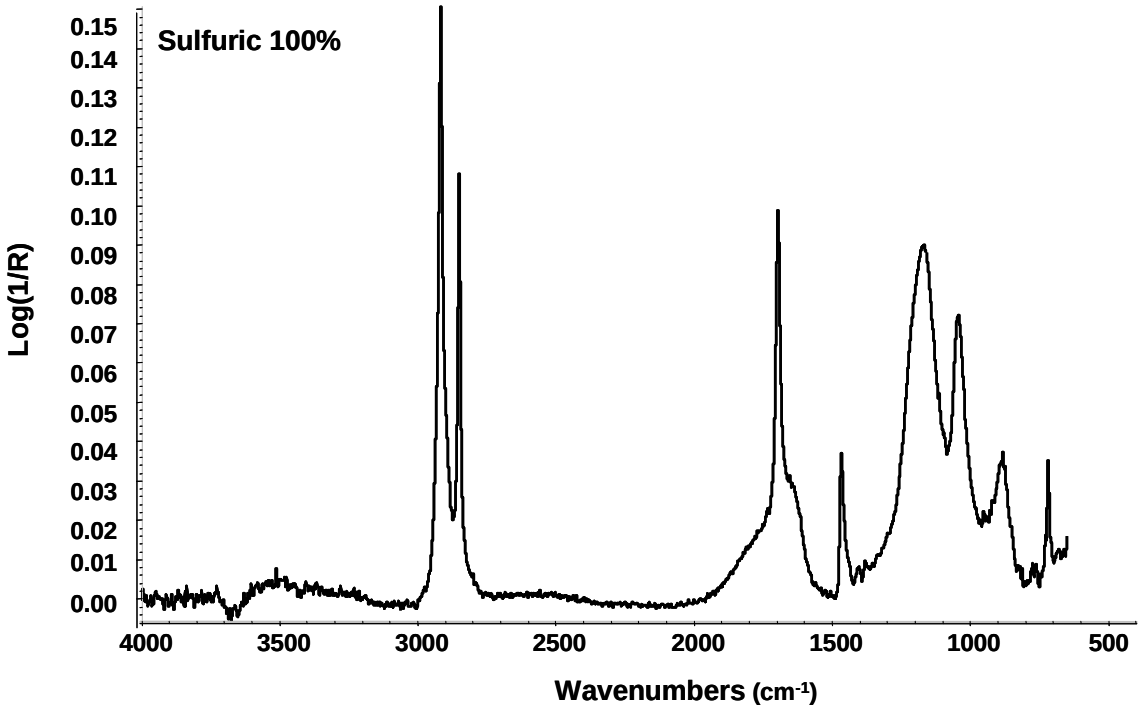


Figure 3-3: Infrared spectrum for the surface of an interlayer sample treated with 100% sulfuric acid solution.

Several concentrations of the sulfuric acid treatments were used to activate the surface of the interlayer samples. Figure 3-4 is a comparison between the untreated interlayer specimen, a 10% sulfuric acid treatment, and a 100% sulfuric acid treatment. It can be observed that the 10% sulfuric acid solution has almost no effect on the surface of the interlayer while the 100% sulfuric acid solution has a very large effect. This suggests that the extent of surface activation depends on the concentration of the treatment being used. An optimal treatment would be one that sufficiently activates the surface of the interlayer without discoloration.

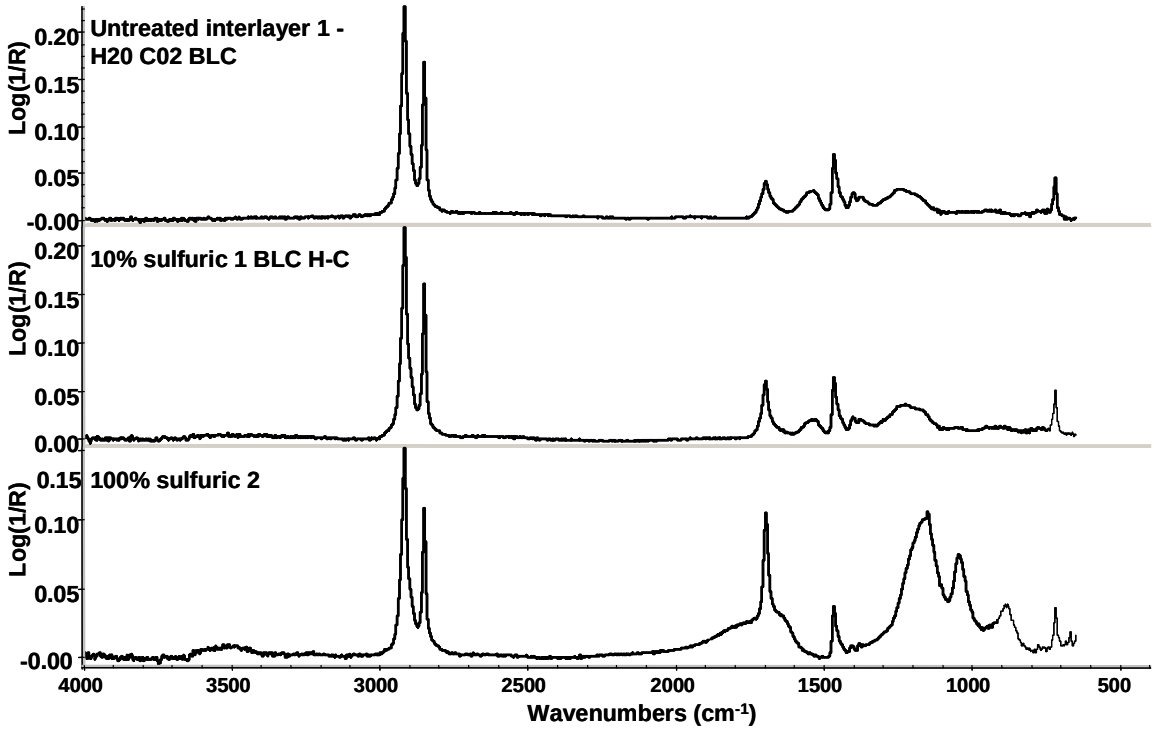


Figure 3-4: Infrared spectrum comparison for interlayer samples a) without acid treatment b) 10% sulfuric acid treatment c)100% sulfuric acid treatment .

A sulfuric acid and nitric acid mixture was also used to treat the surface of the interlayer. This mixture was used to create a strong oxidizing effect on the material surface while preventing discoloration. A comparison between an untreated interlayer, a treatment using 2:1 sulfuric acid to nitric acid, and a treatment using a 3:1 sulfuric to

nitric acid treatment is shown in Figure 3-5. The carbonyl stretch bond is still present on the material surface at comparable concentrations for both samples (concentration is proportional to absorbance). Although there is not a substantial difference in the curves, there was discoloration in the 3:1 sulfuric acid sample.

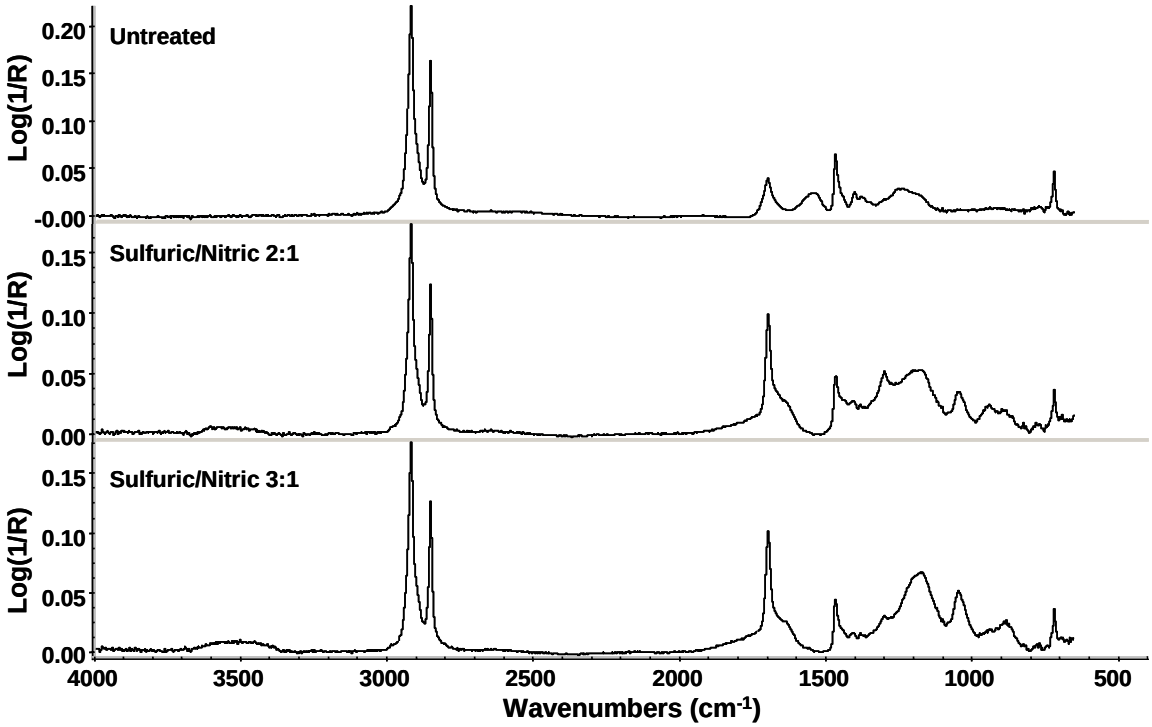


Figure 3-5: Infrared spectrum comparison for interlayer samples a) without acid treatment b) 2:1 sulfuric/nitric acid treatment c) 3:1 sulfuric/nitric acid treatment .

### 3.4.2 Silane Coupling Agent Treatments

All of the silane coupling agents listed above have been used to treat the interlayer samples, but only some were successful based on surface discoloration. Some of the coupling agents caused substantial yellowing and destruction of the sample. The two successful silane coupling agent treatments were 3-aminopropyl trimethoxysilane and N-(2-aminoethyl) 3-aminopropyl trimethoxysilane. Figure 3-7 is an FTIR spectrum comparison for the 3-aminopropyl trimethoxysilane and c N-(2-aminoethyl) 3-aminopropyl trimethoxysilane coupling agents. The most distinguishing characteristic of

these plots is the large peak at 1100 $cm^{-1}$ that corresponds to a Si-OR stretching bond. Since the height of the absorbance peak is proportional to the concentration of bonds on the surface, the sample treated with 3-aminopropyl trimethoxysilane has a large amount of functionalized silane groups on its surface.

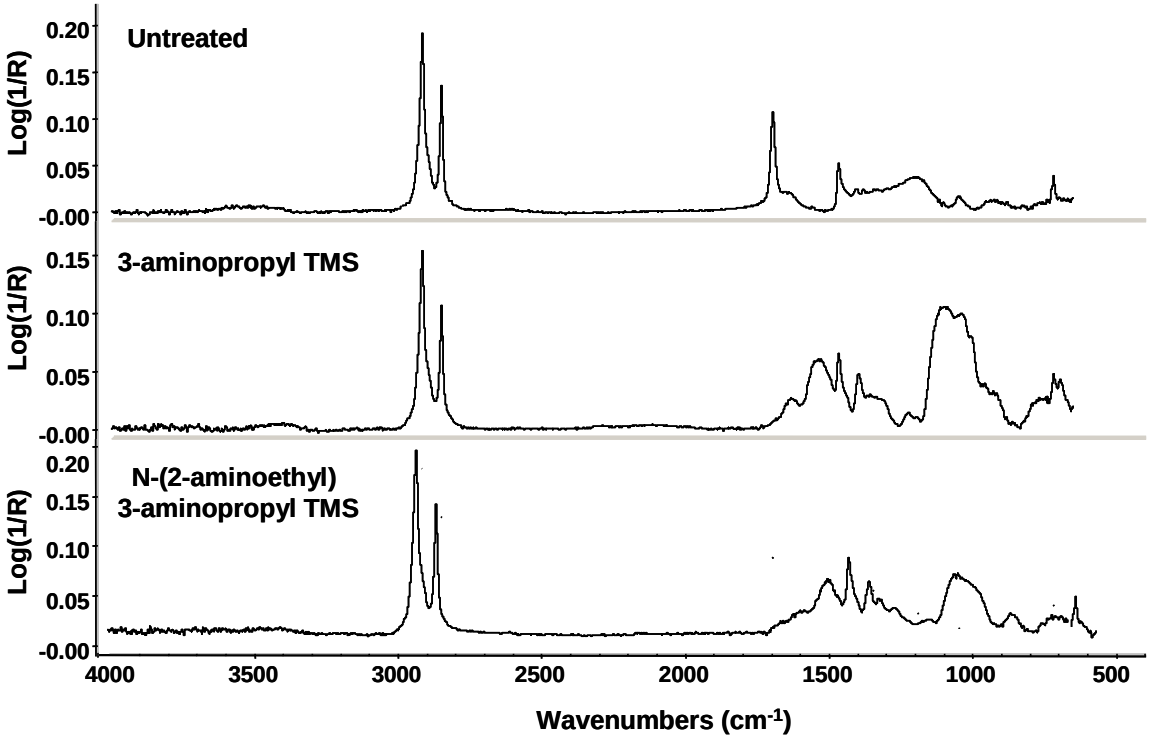


Figure 3-6: Infrared spectrum comparison for interlayer samples a) without silane treatment b) 3-aminopropyl trimethoxysilane treatment c) N-(2-aminoethyl)3-aminopropyl trimethoxysilane treatment .

The absorbance spectrum for N-(2-aminoethyl) 3-aminopropyl trimethoxysilane. The silane peak is not as pronounced for this coupling agent, but the shift in the absorbance peaks suggests that the surface has still been substantially modified.

### 3.4.3. Film Casting onto Treated Interlayer Substrates

The PVA/Laponite dispersions described above were coated onto the substrates of interlayer samples treated with a 2:1 sulfuric/nitric acid treatment and a treatment of 3-aminopropyl trimethoxysilane. These treatments were determined to produce the least

discoloration to the interlayer surface and the most surface change according to FTIR-ATR qualitative analysis. The surfaces treated with 2:1 sulfuric/nitric acid showed the best film adhesion based on visual inspection. The surfaces treated with 3-aminopropyl trimethoxysilane had delamination during the drying process.

# CHAPTER 4
# ABRASION RESISTANT AND ADHESIVE PROPERTIES

## 4.1 Introduction

When formulating an abrasion resistant coating, the performance of the coating depends on several factors. The polymer molecular weight, filler content, drying method, processing temperature, and dispersion rheology can effect the final properties of the protective coating. The scratch resistance and abrasion resistance of protective films are often confused, but maximizing one of these properties may result in a reduction in the other. Abrasion and scratch resistance are related to different material properties. Scratch resistant materials usually have a high hardness and little flexibility. Conversely, abrasion resistant materials depend on the toughness of the coating and are usually flexible and have a high tensile strength.[34-36]

There are several methods for testing the abrasion resistance of coatings. There are several standard test methods for testing abrasion resistance, ASTM D 4060 being the most common.[36] In this method, a Taber Linear Abraser with a grinding wheel is used to abrade a coating on a surface over a fixed amount of time. The weight loss of the coating is measured as a function of number of cycles. The Taber apparatus can be fitted with many different accessories for measuring abrasion resistance, scratch resistance, and color transfer. For smaller samples, such as the samples used in this study, a Taber Linear Abraser (Model 5750) can be used to test small areas and contoured surfaces.

The Taber Linear Abraser can be used to analyze wear resistance of a wide variety of materials. The abrasion tests can be programmed to up to 999,999 cycles with operating speeds of 2, 15, 25, 40, and 60 cycles per minute. The initial load on the specimens is 100 grams, which is loaded by the spline shaft. The load can be increased in 250 gram increments using additional weight discs. The free floating arm has operating stroke lengths of 0.5", 2", 3", and 4", which can be chosen depending on the size of the specimen. The actual abrading of the surface is done by using a wearaser™, which is an abradant made of the same calibrase® and calibrade® material as the grinding wheels that are commonly used. The calibrase® material is resilient and consists of rubber and small abrasive particles. The calibrade® wearaser is non-resilient and is composed of vitrified stone and small abrasive particles.

## 4.2 Materials

Several colloidal dispersions with different Laponite filler content were used to make the multi-layered nanocomposite films. For the samples cast using the doctor blade, a 3 wt% PVA matrix was used with final Laponite loadings of 40, 50, and 60 wt% after drying. This high concentration of PVA is needed for this technique because it will form a gel. A dispersion with a low viscosity would move through the feeder too fast, making it difficult to coat the films uniformly. These multi-layered samples were coated onto extra wide glass slides.

The interlayer samples used were treated with a 2:1 sulfuric to nitric acid solution. The samples were cut into coupons and were coated with PVA concentrations of 1 wt%, 2 wt%, and 3 wt% with Laponite solids loadings corresponding to a dry film concentration of 40 wt%, 50 wt%, and 60 wt% for each PEO concentration. These samples were solution cast and left in a convection oven at 25°C for 24 hours.

Two different wearasers were used to abrade the samples using the Taber Linear Abrader. The CS-10 Calibrase® Wearaser was used to abrade the films mounted on the glass slides. The H-18 Calibrade® Wearaser was used to abrade the single-layered films on the interlayer samples.

## 4.3 Experimental Procedure

### 4.3.1 Sample Preparation

A doctor blade (Richard E. Mistler TTC-1000) was used for tape casting the multi-layered films onto the glass slides. Sufficiently gelled dispersions were loaded into a stationary feeder apparatus that is connected to a moving belt made of silicone coated Mylar. The samples were cast at a speed of 10 inches/minute, which roughly corresponds to a shear rate of 1.41 $s^{-1}$. The films were cast onto wide glass slides and left to dry overnight with air circulating over them. After the first coating, some of the samples were coated again to create a double layer, and some from that group were coated again to form a triple layer.

Interlayer samples treated with a 2:1 sulfuric/nitric acid mixture were coated with nanocomposite films to analyze delamination. Dispersions in 1, 2, and 3 wt% polymer matrices were prepared to cast films with solids loadings corresponding to dry film concentrations of 40, 50, and 60 wt% for each polymer solution. The films were cast in a convection oven at 25°C.

### 4.3.2 Taber Linear Abrader

The experimental methods used for the Taber Linear Abraser are based off of ASTM D 4060. The uncoated and coated glass slides were tested as a function of number of cycles in increments of 10, going from 10-60 cycles using a calibrade® wearaser. The speed was kept constant at 25 cycles per minute with an operating stroke of 1 inch and a

constant load of 100 grams. The samples were secured to the workspace using a metal clamp with cushioning in between to prevent sample breakage. A small brush was used to prevent the accumulation of abraded particles during testing, the samples were continually monitored. The sample weight loss was measured in between each cycle increment.

The method for testing the coated interlayer samples was slightly different due to their tendency to delaminate from the interlayer surface. For this experiment, a calibrase® wearaser was used to abrade the samples for 50 cycles at a stroke length of 1 inch. The load was increased from 100g to 850g in increments of 250 grams using the additional weight discs. If no delamination was observed at the highest load, the speed was increased form 25 cycles/minute to 40 cycles/minute and then to 60cycles/minute. The sample is considered successful if no delamination is observed up to this point.

### 4.3.3 Visual observation of Film Delamination

To obtain a better understanding of the delamination behavior of the nanocomposite films from the interlayer substrate, a visual observation test was conducted on coated interlayer samples. The samples were solution cast with films made from dispersions in 1 wt%, 2wt%, and 3wt% PVA matrices. The films had final solids loadings of 40 wt%, 50 wt%, and 60 wt% for each polymer concentration. The films were cast onto interlayer substrates cut into 1” x 2” coupons and surface treated with a 2:1 sulfuric/nitric acid treatment. To visually observe the delamination of the films from the interlayer substrate, the samples were bent over steel washers of different diameters. A schematic of the washers are shown in Figure 4-1.

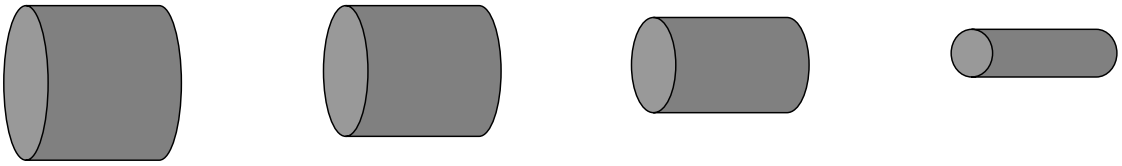


Figure 4-1: Steel rods of different diameters

Each sample was bent over the rods, starting from the largest diamter, and the delamination behavior of the films was recorded.

## 4.4 Discussion of Results

### 4.4.1 Multi-Layered Films

The weight loss data for samples coated with one layer of nanocomposite film are shown in Figure 4-2. The samples are compared to the weight loss of the glass substrate. The sample containing 40 wt% Laponite in the dried film had a weight loss comparable to that of the glass slide. The films containing higher solids loadings had a much larger weight loss, almost triple that of the glass slide. For the coated samples, the clay platelets will be randomly oriented in the film and connected by polymer.[9] The films containing higher solids loading would have less connecting polymer, creating a rougher surface. This rough surface may be easier to abrade than the 40 wt% surface, which would have more polymer connecting the particles. Another observation was that the standard deviation of the film-coated samples were much larger than the standard deviation for the glass slide.

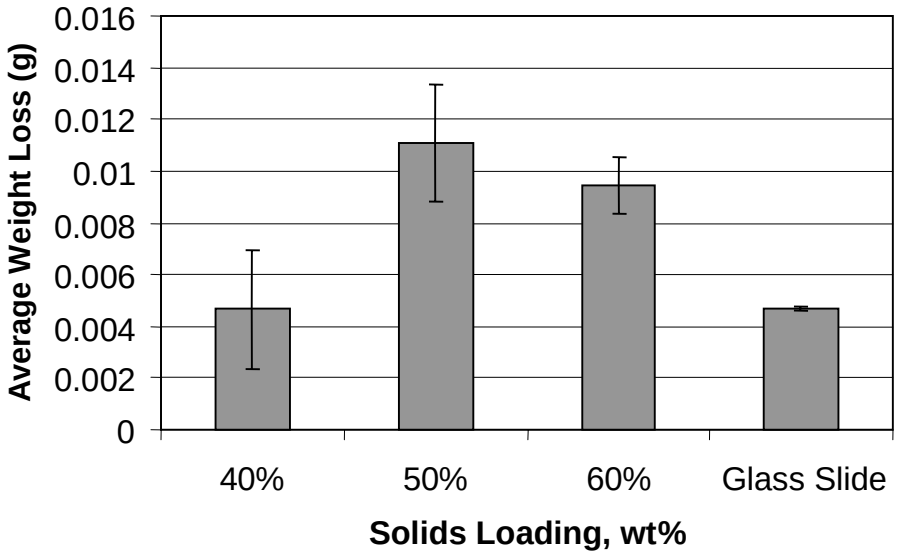


Figure 4-2: Average weight loss data with standard deviation for abraded glass substrate and substrate coated with 40, 50, and 60 wt% nanocomposite films

The weight loss results for the double-coated samples are shown in figure 4-3. In this case, all of the samples performed better than or equal to the glass substrate at resisting weight loss by surface abrasion. Contrary to the single-coating results, the samples containing high solids loadings of Laponite such as 60/50 (60 wt% coated onto 50 wt%), and 50/60 lost the least amount of weight. Additionally, the samples which lost the least amount of weight also have a standard deviation that is much smaller than the samples that lost a larger amount of weight. The samples which have a 40 wt% on the bottom had very large standard deviations, which may be the result of low surface roughness creating a decreased interfacial adhesion to the second layer of film.

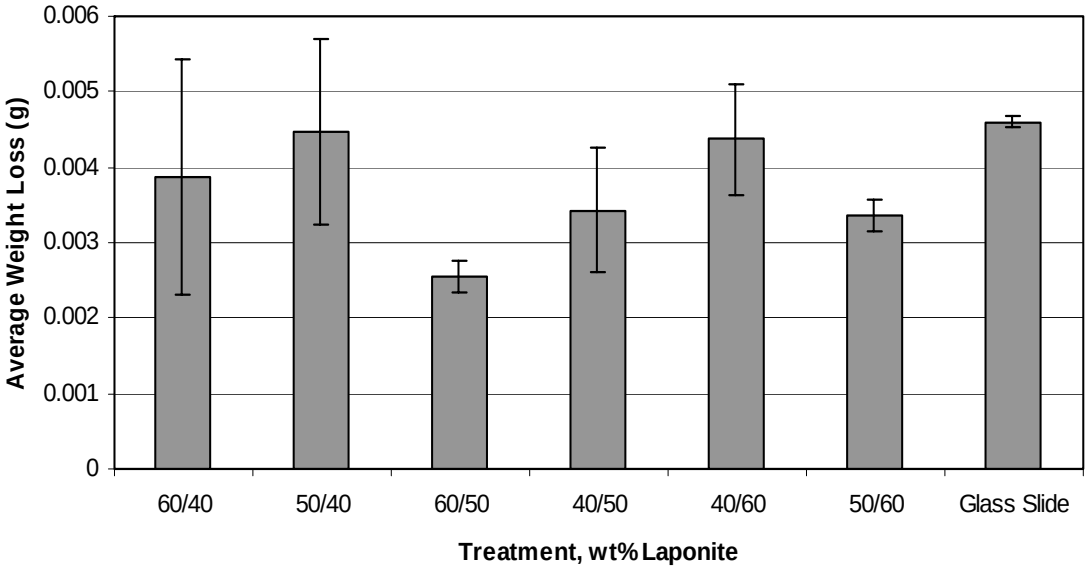


Figure 4-3: Average weight loss data with standard deviation for abraded glass substrate and substrate coated with two layers of nanocomposite film (x/y: film x coated over film y).

Figure 4-4 shows the weight loss results for the triple coated samples. Some of these samples loss less weight than the glass substrate, but several did not perform as well. The samples that had the 40 wt% Laponite film as the top layer (40/50/60 and 40/60/50) lost more weight than the glass and had large standard deviations. As with the double coated samples, this could be due to a decrease in interfacial adhesion between the film layers. The samples with the 60 wt% Laponite film as the top layer performed well but also have high standard deviations. The error in this data is very large, making it difficult to draw conclusions due to an inability to reproduce the results.

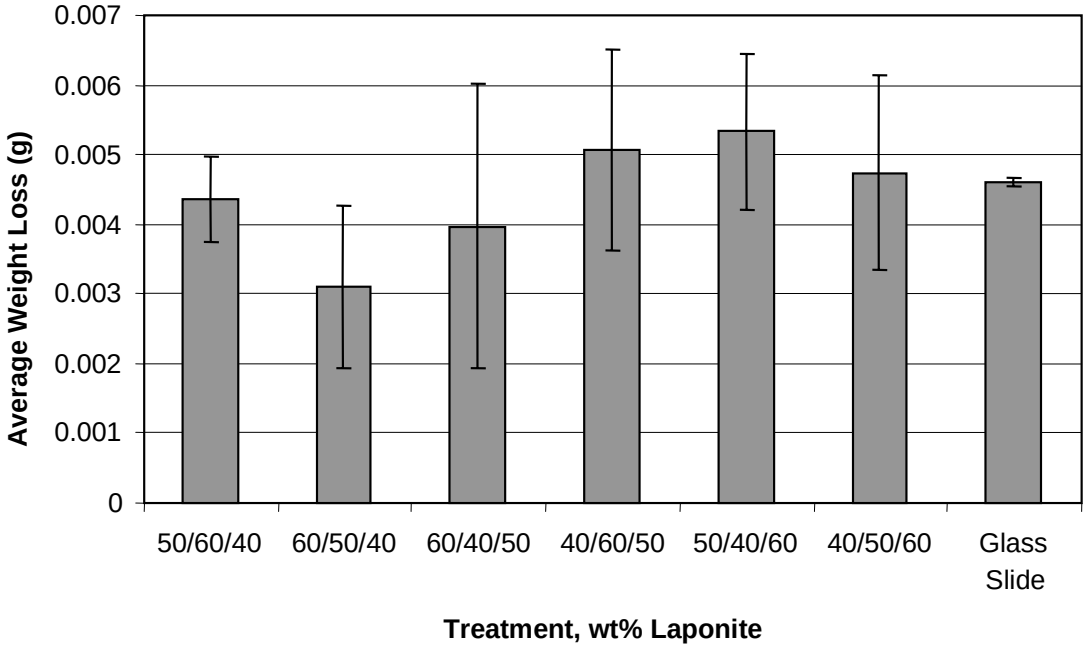


Figure 4-4: Average weight loss data with standard deviation for abraded glass substrate and substrate coated with three layers of nanocomposite film (x/y/z: film x coated over film y coated over film z)

A comparison of the films which loss less than or equal to the amount of weight as the glass substrate are shown in Figure 4-5. All of these coatings are sufficient in providing abrasion resistance that is better than or equal to that of a typical glass specimen. Again it can be seen that the most successful coatings had the smallest standard deviation. When compared to the triple-coated samples, the double-coated samples with films of high solids loading not only lose less weight than the glass slide, but the results are reproducible.

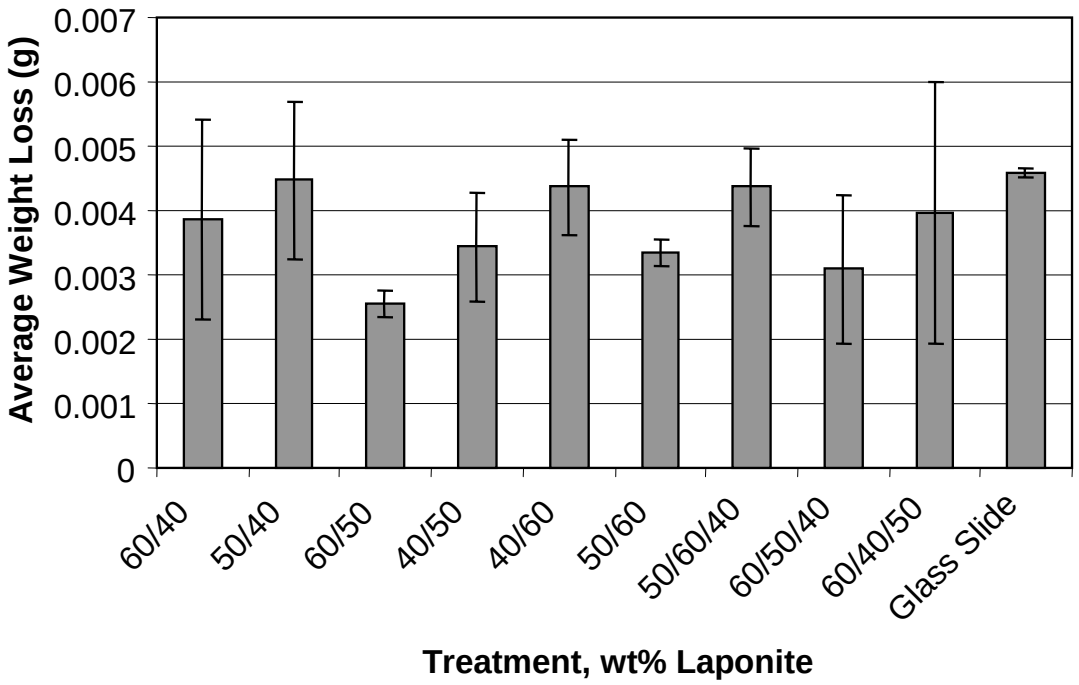


Figure 4-5: A comparison of average weight loss data with standard deviation for the films which loss less than or equal to the amount of weight as the glass substrate

### 4.4.2 Delamination of Coated Interlayer Samples

Upon visual observation, the coated interlayer samples had good adhesion with the nanocomposite film. When abraded by the calibrase® wearaser at different loads and speeds as described earlier, none of the films delaminated from the interlayer surface. Although the Taber instrument was at its maximum capacity, the films were not rubbed from the surface and there was very little haze on the transparent film. Other forms of adhesion testing, such as dynamic mechanical analysis (DMA) or and Instron peel test would provide more insight into the interfacial strength between the films and the treated interlayer substrate.

Visual observation of delamination of the PVA/Laponite films from the interlayer substrate was achieved with the steel rod test. All of the film samples prepared

in a 1 wt% PVA matrix did not delaminate when bent over the rods. Even the smallest diameters did not succeed in changing the appearance of the film or adhesion to the substrate. The films prepared in 2 wt% PVA dispersions did not fracture from the interlayer surface, but they did delaminate. The film with the lowest solids loading (40 wt%) was not effected by the larger diameters, but at 1.27cm the film/interlayer interface turned white, suggesting the film was peeling from the surface. The 50 and 60 wt% films had this same behavior on the 1.9cm rod. The films cast in a 3 wt% PVA matrix fractured on the largest diameter rod. When bent, they fractured along the middle of the sample and continued to peel back if bent further. Larger rods would be needed to define the point where fracture occurs for these films.

# CHAPTER 5
# CONCLUSIONS AND FUTURE WORK

## 5.1 Conclusions

When Laponite JS is dispersed in water, it can form a stable sol which exhibits Newtonian behavior. When polymer is present, the interactions between the polymer chains and the particles cause a change in the rheological properties of the dispersions. As polymer dosage is increased in a Laponite dispersion, particle flocculation causes a weak colloidal gel to form and the viscosity increases. Shear thinning behavior can be seen for these colloidal gels at high shear rates, noting a breakdown and particle alignment in the weakly flocculated network structure. SEM analysis shows that the flocs present in the dispersions are open, ramified structures that are evenly dispersed throughout the dispersions. The flocs are not interconnected, which makes it easier for structural breakdown to occur at high shear rates and high angular frequencies.

The processing conditions for films made from 2 wt% and 3 wt% PVA solutions include Newtonian-like behavior at low shear rates and shear thinning behavior at high shear rates. For the 2 wt% PVA dispersions, the weakly flocculated gel structure can be broken down at high frequencies; this does not occur for dispersions made in a 3 wt% PVA matrix. For low shear processing techniques like solution casting, a 2 wt% PVA matrix is ideal; the 3 wt% PVA matrix would work for high shear techniques such as tape casting and spin coating.

The processing conditions of the colloidal gels are determined as a function of both solids loading and polymer concentration. An increase in solids loading at fixed

PVA concentration causes a shift in zero shear viscosity and an increase in the shear rate dependent region of the steady-shear viscosity curves. The effect of the suspending fluid is crucial in the processing of the coatings due to the large increase in viscosity with increasing PVA concentration.

Thin, transparent films can be cast from the PVA/Laponite dispersions. These films exhibit good adhesion to glass slides, but cannot be cast onto a hydrophobic polymer interlayer. To activate the surface of the interlayer, and reduce the surface tension, several surface treatments were used. Using FTIR-ATR, it can be observed that several of these treatments can successfully activate the interlayer surface. A 100% sulfuric acid treatment will activate the surface, but will create substantial yellowing. A mixture of sulfuric and nitric acid in a ratio of 2:1 will also activate the surface but will not cause discoloration. This treatment showed a substantial improvement in adhesion between the cast films and the interlayer substrate. Silane coupling agents will also successfully modify the interlayer surface, but it was observed that the interfacial adhesion to the nanocomposite films was not improved.

To determine the abrasion resistance of cast nanocomposite films on glass slides, a Taber Linear Abrader was used determine weight loss as a function of number of cycles. Coatings with one, two, and three layers of film at different solids loading were tested for weight loss against an uncoated glass slide specimen. The single coated samples did not perform as well as the glass slide, i.e. they lost more weight than the glass. The double coated samples performed better than the glass slide at every solids loading, with the highest solids loadings (50/60 and 60/50) losing the most weight. With the triple coated samples, only some lost less weight than the glass slide. In conclusion,

the optimal coating for the glass to minimize weight loss and maximize efficiency is a double-layered film of high solids loading.

## 5.2 Future Work

The field of polymer-layered silicate nanocomposites is very large and has a broad range of applications. Further study of the PVA/Laponite JS system and systems with similar properties is useful to assess their use in the films and coatings industry. For use as an abrasion resistant film, more mechanical and thermal analysis of the material must be performed. Adhesion is a large concern for this application and maximizing this property would be useful. The following are suggestions for possible future work.

- To further determine the abrasion resistant properties of the films, mechanical studies can be conducted on interlayer samples coated with various PVA/Laponite films. These studies would include Instron tensile testing and dynamic mechanical analysis. Since tensile strength is proportional to abrasion resistance, an optimal formula can be determined.
- To continue rheological studies on the PVA/Laponite system, an in-depth study on the structural development of the dispersions can be conducted.
- Perform surface activation of the polymer interlayer surface using RF plasma treatment. This treatment is more expensive than wet-chemical treatments and requires special equipment, but may be more effective in creating an activated polymer surface.
- When used as a laminated glass, the SentryGlas ionomer is heat treated and becomes a harder, more glass-like material. This glassy polymer is adhered to window glass to improve the properties of the window. Analysis can be done on the surface of heat treated interlayer using contact angle measurements and FTIR-ATR.
- UV-VIS experiments can be performed on glass, film-coated glass, and abraded materials to determine the transparency of the films compared to regular window glass. The effect of abrasion on the transparency of the glass can also be determined using this technique.
- Using different materials for both the polymer matrix and the nanosilicate can be used to continue this investigation. Some possible polymers would be Poly Methyl Methacrylate (PMMA), Poly Ethylene Oxide (PEO), Polycarbonate (PC), and polyvinyl acetate (PVA). Also, different grades of Laponite can be used as the nanosilicate filler.

LIST OF REFERENCES


1. A.R.Vaia.; R. Krishnamoorti, 2001. Polymer nanocomposites: introduction. ACS Symposium Series 804. Materials and Manufacturing Directorate, Air Force Research Library, 2001.

2. J. Collister, 2001. Commercialization of polymer nanocomposites. ACS Symposium Series 804. Edison Polymer Innovation Corporation.

3. S. Bandyopadhyay; A. J. Hseih. E. P. Giannells. 2001. PMMA Nanocomposites synthesized by emulsion polymerization. ACS Symposium Series 804.

4. B. Wetzel; F. Hauper; K. Friedrich; M. Zhang; M. Rong. Impact and wear resistance of polymer nanocomposites at low filler content. Polymer Engineering and Science, September 2002.

5. M. Alexandre, P. Dubois. Polymer-layered silicate nanocomposites: preparation, properties, and uses of a new class of materials. Materials Science and Engineering 28 (2000) 1-63.

6. J. Zebrowski, V. Prasad, W. Zhang, L.M. Walker, D.A. Weitz. Shake-gels: shear-induced gelation of Laponite-PEO mixtures. Colloids and Surfaces A: Physicochem. Eng. Aspects 213 (2003) 189.

7. S. Lin-Gibson, H. Kim, G. Schmidt, C.C. Han, E.K. Hobbie, J. Shear-induced structure in polymer-clay nanocomposite solutions. Colloid Interface Sci. 274 (2004) 515.

8. D. C. Pozzo, L.M. Walker. Reversible shear gelation of polymer-clay dispersions. Colloids and Surfaces 240 (2004) 187-198.

9. V. Ferreiro, G. Schmidt, C. Han, A. Karim. Dispersion and nucleating effects of clay fillers in nanocomposite polymer films. Polymer Nanocomposites: Synthesis, Characterization, and Modeling (2002) 177.

10. A. Nelson, T. Cosgrove. A small-angle neutron scattering study of adsorbed poly (ethylene oxide) on Laponite. Langmuir 20 (2003) 2298.

11. G. Schmidt, M. Malwitz. Properties of polymer-nanoparticle composites. Curr. Opin. Colloid Interface Sci. 8 (2003) 103.

12. Ronald G. Larson. The structure and rheology of complex fluids. Oxford University Press, New York, 1999.

13. Rockwood Additives Ltd., Cheshire, United Kingdom. Laponite Technical Bulletin L204/01g

14. R. Krishnamoorti, K. Yurekli. Rheology of polymer layered silicate nanocomposites. Curr. Opin. Colloid Interface Sci. 6 (2001) 464.

15. J. Labanda, J. Llorens. Rheology of Laponite colloidal dispersions modified by sodium polyacrylates. Colloids and Surfaces A: Physiochem. Eng. Aspects 249 (2004) 127-129.

16. M. Malwitz, A. Dundigalla, V. Ferreiro, P. Butler, M.C. Henk, G. Schmidt. Layered structures of shear-oriented and multilayered PEO/silicate nanocomposite films. Phys. Chem. 6 (2004) 2977.

17. J. Ren, B. Casanueva, C.A. Mitchell, R. Krishnamoorti. Disorientation kinetics of aligned polymer layered silicate nanocomposites. Macromolecules 36 (2003) 4188.

18. Z. Shen, J. Chen, H. Zou, J. Yun. Rheology of colloidal nanosized BaTiO3 suspension with ammonium salt of polyacrylic acid as a dispersant. Colloids and Surfaces 244 (2004) 61-66.

19. M. Sjoberg, L. Bergstrom, A. Larsson, E. Sjostrom. The effect of polymer and surfactant adsorption on the colloidal stability and rheology of kaolin dispersions. Colloids and Surfaces 159 (1999) 197-208.

20. J. A. Lee, M. Kontopoulou, J. S. Parent. Time and shear dependent rheology of maleated polyethylene and its nanocomposites. Polymer (2004) 1-6.

21. S. Granick, H. Hu, G.A. Carson. Nanorheology of confined polymer melts. 2. nonlinear shear response at strongly adsorbing surfaces. Langmuir 10 (1994) 3867.

22. A. Mukhopadhyay, S. Granick. Micro- and nanorheology. Curr. Opin. Colloid Interface Sci. 6 (2001) 423.

23. J. Bergenholtz. Theory of rheology of colloidal dispersions. Curr. Opin. Colloid Interface Sci. 6 (2001) 484

24. P. Mongondry, T. Nicolai, J. Tassin. Influence of pyrophosphate or polyethylene oxide on the aggregation and gelation of aqueous laponite dispersions. J. Colloid Interface Sci. 275 (2004) 191.

25. S. Carra, A. Sliepcevich, A. Canevarolo, S. Carra. Grafting and adsorption of poly (vinyl) alcohol in vinyl acetate emulsion polymerization. Polymer 46 (2005) 1379-1384.

26. A. A. Zaman, N. Delorme. Effect of polymer bridging on rheological properties of dispersions of charged silica particles in the presence of low-molecular-weight physically absorbed poly (ethylene oxide). Rheol Acta 41 (2002) 408-417.

27. A. A. Zaman, M. Bjelopavlic, B.M. Moudgil. Effect of adsorbed polyethylene oxide on the rheology of colloidal silica suspensions. J. Colloid Interface Sci. 226 (2000) 290-298.

28. R. Chanamai, D. J. McClements. Creaming stability of flocculated monodisperse oil-in-water emulsions. J. Colloid Interface Sci. 255 (2000) 214-218

29. H. Anderlean, S. Petit, P. Laurens, P. Marcus, F. Arefi-Khonsari. Effects of different laser and plasma treatments on the interface and adherence between evaporated aluminum and polyethylene terepthalate films: X-ray photoemission and adhesion studies. Applied Surface Science 243 (2005) 304-318.

30. Jasco, Inc., Easton, MD. IR Application Note 02-03. Qualitative analysis of powdered solids with FTIR-ATR.

31. A.K. Pal, R.K. Roy, S.K. Randal, S. Gupta, B. Deb. Electrodeposited carbon nanotube thin films. Thin Solid Films 476 (2005) 288-294

32. Y.H. Wang, R. Kumar, X. Zhou, J.S. Pan, J.W. Chai. Effect of oxygen plasma treatment on low dielectric constant carbon-doped silicon oxide thin films. Thin Solid Films 473 (2005) 132-136.

33. J.E. Klemberg-Sapieha, L. Martinu, N.L.S Yamasaki, C.W. Lantman. Tailoring the adhesion of optical films on polymethyl-methacrylate by plasma-induced surface stabilization. Thin Solid Films 476 (2005) 101-107

34. D. H. Jeong, U. Erb, K. T. Aust, G. Palumbo. The relationship between hardness and abrasive wear resistance of electrodeposited nanococrystalline Ni-P coatings. Scripta Materiala 48 (2003) 1067-1072

35. S. Suzuki, E. Ando. Abrasion of thin films deposited onto glass by the Taber test. Thin Solid Films 340 (1999) 194-200

36. L. Dulany, 2002. Scratch- and abrasion-resistant coatings with energy-curable resin samples. UCB Chemicals Corp., Smyrna, GA.

# BIOGRAPHICAL SKETCH

The author was born in Havertown, Pennsylvania, a small suburb outside of Philadelphia. She obtained her high school diploma from Cypress Creek High School in Orlando, Florida. She went on to get her bachelor's degree in materials science and engineering at the University of Florida in Gainesville, where she was active in the Benton Engineering Council and the Materials Research Society. She continued her education at the University of Florida to pursue a Master of Science in materials science and engineering. She worked with Dr. Abbas Zaman during undergraduate and graduate studies on colloidal systems and polymer thin films.